ORNL/TM-2004/123

Nuclear Science and Technology Division

PRODUCTION OF DEPLETED UO_2 KERNELS FOR THE ADVANCED GAS-COOLED REACTOR PROGRAM FOR USE IN TRISO COATING DEVELOPMENT

J. L. Collins
R. D. Hunt
G. D. Del Cul
D. F. Williams

Date Published: November 2004

Prepared by
OAK RIDGE NATIONAL LABORATORY
P.O. Box 2008
Oak Ridge, Tennessee 37831-6285
managed by
UT-BATTELLE, LLC
for the
U.S. DEPARTMENT OF ENERGY
under contract DE-AC05-00OR22725

CONTENTS

Page

LIST OF FIGURES

LIST OF TABLES

ACRONYMS

AAA	Advanced Accelerator Application (Program)
ADUN	acid-deficient uranyl nitrate
AGR	Advanced Gas-Cooled Reactor
DOE	U.S. Department of Energy
DTA	differential thermal analysis
HMTA	hexamethylenetetramine
ICP-MS	inductively coupled plasma–mass spectroscopy
ORNL	Oak Ridge National Laboratory
PVC	polyvinylchloride
SEM	scanning electron microscopy
TCE	trichloroethylene
TGA	thermogravimetric analysis
TRISO	triisotropic

ACKNOWLEDGMENTS

The UO_2 kernel production work was sponsored by the U.S. Department of Energy, Office of Nuclear Energy, Science and Technology, under the Nuclear Energy Technologies Program and the Advanced Fuel Cycle Initiative Program under contract DE-AC05-00OR22725 with UT-Battelle, LLC.

The efforts of other ORNL staff are greatly appreciated. The crafts personnel and the instrument technicians of the Facilities and Operations Directorate did an excellent job in constructing and installing the gel-forming apparatus in the radiological hoods. Chris Grainger and Frank Barrera of the Operational Safety Services Division provided excellent support for this work. The authors also appreciate Gary Bell, Ben Lewis, Dave Hill, and Jim Rushton for their managerial support; Barry Spencer and Roger Spence for their helpful technical reviews; Brenda Johnson for preparation of the document; and Marsha Savage for editing.

ABSTRACT

The main objective of the Depleted UO_2 Kernels Production Task at Oak Ridge National Laboratory (ORNL) was to conduct two small-scale production campaigns to produce 2 kg of UO_2 kernels with diameters of 500 ± 20 μm and 3.5 kg of UO_2 kernels with diameters of 350 ± 10 μm for the U.S. Department of Energy Advanced Fuel Cycle Initiative Program. The final acceptance requirements for the UO_2 kernels are provided in the first section of this report. The kernels were prepared for use by the ORNL Metals and Ceramics Division in a development study to perfect the triisotropic (TRISO) coating process. It was important that the kernels be strong and near theoretical density, with excellent sphericity, minimal surface roughness, and no cracking.

This report gives a detailed description of the production efforts and results as well as an in-depth description of the internal gelation process and its chemistry. It describes the laboratory-scale gel-forming apparatus, optimum broth formulation and operating conditions, preparation of the acid-deficient uranyl nitrate stock solution, the system used to provide uniform broth droplet formation and control, and the process of calcining and sintering $UO_3 \cdot 2H_2O$ microspheres to form dense UO_2 kernels. The report also describes improvements and best past practices for uranium kernel formation via the internal gelation process, which utilizes hexamethylenetetramine and urea. Improvements were made in broth formulation and broth droplet formation and control that made it possible in many of the runs in the campaign to produce the desired 350±10-μm-diameter kernels, and to obtain very high yields.

A total of 45 gel-forming preparations were made to produce 2 kg of the 500±20-μm-diameter UO_2 kernels, which were then combined into two lots. A total of 1630 g of kernels were sieved between 500 ± 2 μm and 534 ± 2 μm with ASTM E161 electroformed sieves, while 386 g were sieved between 482 ± 2 μm and 518 ± 2 μm (also with ASTM E161 electroformed sieves). Both batches of kernels were separately mixed well and riffled into 100-g samples. One of the samples (DUN 500-S-1) from the larger batch was analyzed by the Metals and Ceramics Division characterization laboratory at ORNL. The kernels had an average mean diameter of 519 μm with a standard deviation in the distribution of 12 μm. The mean diameter of the 1.6-kg batch of kernels was 519 ± 1 μm with 95% confidence, with <1% of the measured kernels outside the range 500–545 μm. The average sphericity was 1.020 with a standard deviation of 0.008. The mean sphericity of the 1.6-kg batch of kernels was 1.02 ± 0.01 μm with 95% confidence. The distribution was skewed toward higher sphericity, with <0.5% of the measured kernels having a sphericity >1.05. The envelope density, as measured with a mercury porosimeter, was 10.6 g/cm^3 with an open porosity of ~1%. The skeletal density, which was measured with a helium pycnometer, was 10.82 ± 0.16 g/cm^3. The average values for the tap and slow-pour densities were 6.68 and 6.69 g/cm^3, respectively.

Ninety-two production runs were made to obtain 3.4 kg of the 350±10-μm-diameter kernels. For the broader size diameter tolerance of 350 ± 20 μm, about 4 kg of kernels were produced. The average skeletal density for a sample of the kernels, as measured via a helium pycnometer, was 10.85 g/cm^3 (~99% of the theoretical density). The average slow-pour density was 6.69 g/cm^3.

Analyses for cations and chloride in samples of kernels from each of the campaigns found that the concentrations of the contaminants were well within the final acceptance

criterion of ≤50 μg/g with 95% confidence. For a sample of 500-μm kernels, the only cations reported that were above the detection limit were as follows: 33.6 ± 3.4 μg/g Ni, 11.6 ± 1.2 μg/g Al, 10.7 ± 1.1 μg/g Ca, 10.6 ± 1.1 μg/g Cu, and 5.6 ± 0.6 μg/g Cr. For a sample of 350-μm kernels, detection limits were exceeded as follows: 15.6 ± 1.6 μg/g K, 13.4 ± 1.3 μg/g Cr, 6.3 ± 0.6 μg/g Fe, 5.4 ± 0.4 μg/g Mg, 5.1 ± 0.5 μg/g Al, 4.5 ± 0.5 μg/g Ni, and 2.7 ± 0.3 μg/g Cu. In separate analyses for chloride of samples of the 500- and 350-μm kernels, the concentrations were in the acceptable range, with the highest value being 35 μg/g.

1. INTRODUCTION

1.1 Goals of Depleted UO_2 Kernels Production Task

The goal of the Depleted UO_2 Kernels Production Task of the Advanced Gas-Cooled Reactor (AGR) Program was to prepare 2 kg of UO_2 kernels with diameters of 500 ± 20 μm and 3.5 kg of UO_2 kernels with diameters of 350 ± 10 μm for use by the Metals and Ceramics Division at Oak Ridge National Laboratory (ORNL) in the triisotropic (TRISO) coating development. The objective was to produce sintered UO_2 kernels that were suitable for TRISO coating that were strong and near theoretical density, with excellent sphericity, minimal surface roughness, no cracking, and good crush strength. The final acceptance requirements for the depleted UO_2 kernels for use in coating development are shown in Table 1.

Table 1. Final acceptance requirements for the UO_2 kernels
(All values represent 95% confidence level)

Property	Mean
Individual impurities (Li, Na, Ca, V, Cr, Mn, Fe, Co, Ni, Cu, Zn, Al, Cl), ppm wt	≤50
Total impurities (Li, Na, Ca, V, Cr, Mn, Fe, Co, Ni, Cu, Zn, Al, Cl), ppm wt	≤1000
Kernel density, g/cm^3	≥10.7
Diameter, μm	350 ± 10
Diameter, μm	500 ± 20

The internal gelation process was chosen as the means to prepare the gel spheres that could be calcined and sintered to obtain the targeted kernels.

1.2 Internal Gelation Process and Its Chemistry

The internal gelation process used at ORNL was originally developed at the KEMA laboratory located in the Netherlands.[1] Since the late 1970s, researchers at ORNL have studied and fully developed the internal gelation process for making UO_2, $(U,Pu)O_2$, ThO_2, and $(UO_2 + UC_2)$ microspherical fuels.[2-18] The internal gelation process used is one of the sol-gel processes developed for the preparation of microspheres of nuclear fuel in which chilled clear broth droplets containing acid-deficient uranyl nitrate (ADUN), hexamethylenetetramine (HMTA), and urea are heated causing homogenous gelation and solidification of the droplets that, after washing treatments, can be dried calcined, and sintered to ceramic kernels of the required density. In the 1990s, ORNL researchers extended the boundaries of the technology by developing the process to make hydrous metal oxide spheres of Ti, Zr, Fe, and other cations for such uses as sorbents, waste forms, catalysts, getters, and dielectrics.[19-22]

The advantages of the internal gelation process for nuclear fuel kernels of uranium include the following: (1) control of gelation time and microsphere size, (2) reproducible preparations, (3) control of uranium crystal morphology in the gel

spheres, (4) homogeneous incorporation of fine particles of other materials into the microspheres, and (5) a highly developed large-scale engineering process. To maximize these advantages, the preparation of urania kernels requires a detailed understanding of the gel-forming process chemistry operation. Several of the process parameters significantly impact the quality of the kernels.[9,11] The crystal morphology and the concomitant microsphere properties are significantly affected by the (1) HMTA/U mole ratio, (2) NO_3^-/U mole ratio, (3) gel-forming temperature, and (4) HMTA-urea feed preparation method. Subsequent aging and air-drying also impact crystallite growth.

Broth droplets in which the NO_3^-/U mole ratio is between 1.5 to 1.7 that are heated at temperatures of 50 to 70°C yield gel spheres that are considerably less dense than those obtained using similar broths that are heated in the temperature range 70 to 95°C. The density can vary by as much as a factor of 2. A sharp contrast is also noted in the color of these gel spheres, with intensities varying from pale yellow for the ones with the lowest densities to golden yellow to orange for those with the highest densities. These colors and densities are indicators of the crystal morphology and porosity. Those that are pale yellow (i.e., with the lowest density) have the largest crystals and the largest pores. Conversely, those that are golden yellow to orange and have high densities have small crystals and pores or are amorphous. Gel spheres that have extremely large crystals and pores tend to be weaker and experience more surface leaching and erosion during the washing steps. Gel spheres that are amorphous or have the smallest crystals and pores are stronger, but the reaction impurities are much more difficult to remove during the washing steps. This latter group of spheres is more prone to crack during the drying, calcining, and sintering steps.

In a study by M. H. Lloyd et al.,[2] transmission electron microscopy and X-ray diffraction analyses showed that the variations in the gel-forming properties yielded gel spheres with a wide range of crystallite structures and compositions. The uranium phases consisted of thin platelets of diameters varying from ~100 to 5000 Å. The packing density varied greatly with the diameter of the platelets because of the distinctive platelet structure of the urania. Extensive X-ray diffraction analyses found three different compounds in the $UO_3 - NH_3 - H_2O$ system: (1) $UO_3 \cdot 2H_2O$, (2) $UO_3 \cdot 1/4NH_3 \cdot 7/4H_2O$, and (3) $2UO_3 \cdot NH_3 \cdot 3H_2O$. Compound 1 contained primarily large crystals with diameters in the 1000- to 5000-Å range. The crystals of compound 2 were small, in the 100- to 200-Å range. The NH_3 was associated with small crystals. Compound 3 contained phases of both compounds 1 and 2. Noncrystalline or distinctively amorphous material as well as mixed crystalline–amorphous material was also found in some preparations.

The goal of the kernel fabrication task was to produce sintered kernels that were suitable for TRISO coating. The kernels had to be strong and near theoretical density, with excellent sphericity, minimal surface roughness, no cracking, and good crush strength. Optimum operating conditions and broth formulation were determined that yielded gel spheres in which the size of the crystals and pores were in the midrange (based upon past experience). The tap density for these air-dried spheres ranged from 1.08 to 1.2 g/cm^3.

The following four key reactions are important in the chemistry of the internal gelation process. In the process, a clear broth is formed when a chilled solution of concentrated HMTA and urea is mixed with a chilled concentrated solution of ADUN. Depending on the NO_3^-/U mole ratio (a measure of the acid deficiency), the pH of the

broth can vary from 3.5 to 6. Under normal conditions, uranium precipitation occurs at a pH ≥3.25; however, the urea in the broth forms a complex with the uranyl ions [reaction (1)] and prevents precipitation from occurring at the lower temperatures (0 to 10°C). When the droplets of broth are introduced into a heated stream of immiscible organic medium like silicone oil or trichloroethylene (TCE), decomplexation [the reverse of reaction (1)] occurs, allowing hydrolysis [reaction (2)] to proceed. The HMTA in the broth is a weak organic base that readily consumes the H^+ that is generated by reaction (2). This process occurs via HMTA protonation [reaction (3)] and protonated HMTA decomposition [reaction (4)], resulting in the precipitation and gelation of the uranium. Urea in the heated broth plays another major role. It acts as a catalyst by causing the decomposition of protonated HMTA molecules, which results in the HMTA becoming a more effective base. However, decomposition occurs only after most of the HMTA molecules have been protonated.[11]

1. **Complexation/Decomplexation**
   $2CO(NH_2)_2 + UO_2^{2+} \leftrightarrow UO_2[CO(NH_2)_2]_2^{2+}$

2. **Hydrolysis**
   $UO_2^{2+} + xH_2O \leftrightarrow UO_2(OH)_2\bullet(x-2)H_2O + 2H^+$

3. **HMTA Protonation**
   $(CH_2)_6N_4 + H^+ \leftrightarrow (CH_2)_6N_4\bullet H^+$

4. **Protonated HMTA Decomposition**
   $(CH_2)_6N_4\bullet H^+ + 3H^+ + 6H_2O \leftrightarrow 4NH_4^+ + 6CH_2O$

2. LABORATORY-SCALE APPARATUS AND ITS OPERATION

The laboratory-scale apparatus (Fig. 1) that was used to make the hydrous uranium oxide gel spherules in this program was a modification of an apparatus used to produce uranium and plutonium microspheres in a glove box in the late 1970s.[15] The apparatus consisted of a reservoir for heating the silicone oil (Dow Corning 200 silicone fluid), a pump for circulating the silicone oil through the gel-forming apparatus, a chilled broth pot, a vibrating nozzle system for controlling the size of the broth droplets, a glass gel-forming column (see Fig. 2), a downstream polyvinylchloride (PVC) transport line to provide a residence time for the gel spherules to hydrolyze and solidify, and a stainless steel mesh product collector for collecting and aging the gel spheres and also for separating the silicone oil from the spheres.

The silicone oil reservoir was a stainless steel open-top rectangular container that was 7 in. wide by 8.3 in. long and 11.5 in. deep. Two 250-W stainless steel heating blades were positioned at the rear of the reservoir to heat the oil. A thermocouple that was positioned in the basket at the bottom and near the front of the reservoir was connected to a temperature controller, which was used to control the temperature of the oil. A Lightnin® mixer with its stainless steel shaft positioned between the two heating blades and its stainless steel impeller located near the bottom of the reservoir was used to

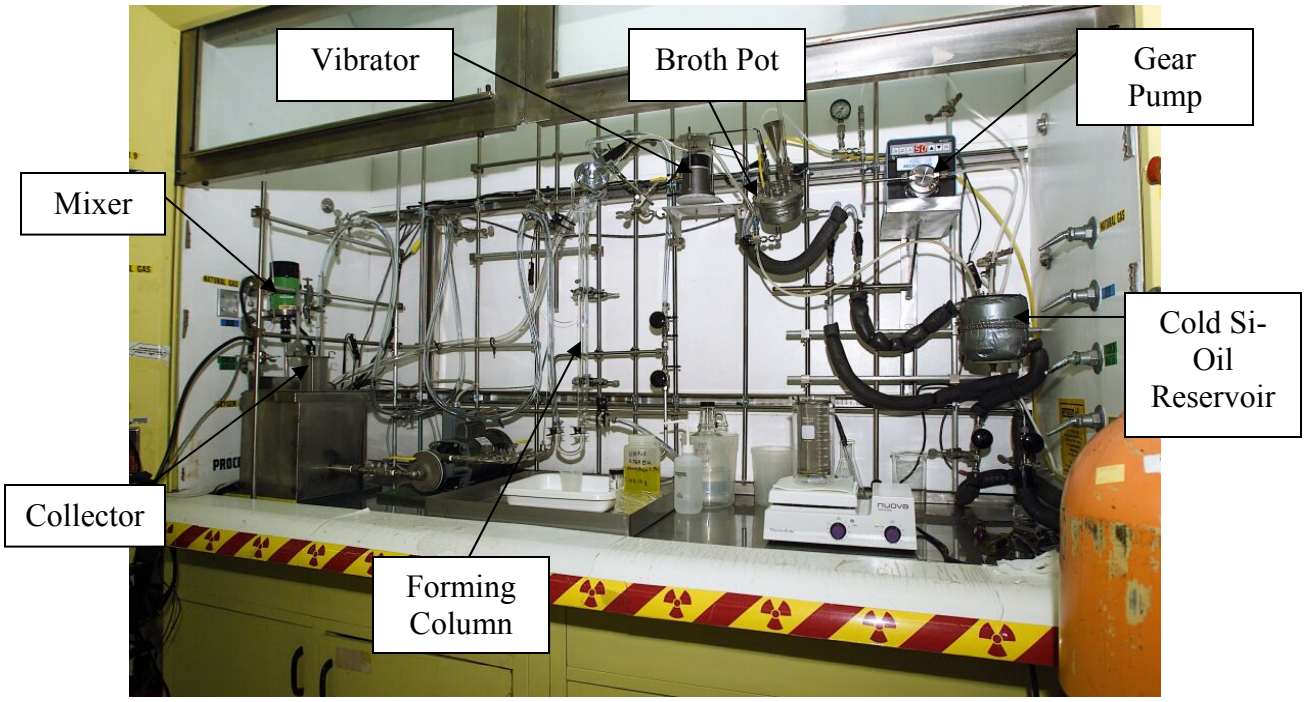

Fig. 1. Laboratory-scale apparatus used to prepare $UO_3 \cdot 2H_2O$ gel spheres.

mix and maintain the oil at the desired temperature. Taking up most of the space at the front of the reservoir was a large removable stainless steel wire-mesh (100-mesh) basket, which served as a backup to prevent any spilled gelled spherules from being pumped out of the reservoir to the circulating pump. An Eastern D-centrifugal pump was used to pump the hot oil from the reservoir through a 1/4-in.-ID stainless steel line to the vertically positioned glass gelation column. The flow from the pump was divided into two streams, which were controlled by manual valves. The flow of one of the streams was routed to a position that was above the top of the gelation column (see Fig. 2) to a 3/8-in.-OD stainless steel, dead-end tube with a narrow slit, which was used to form a veil of silicone oil that was directed into the entrance of the gelation column (see Fig. 2). The slit (1.25 in. long and 0.016 in. wide) was normally positioned ~1 in. above the entrance to the column. It formed a V-shaped veil of silicone oil, whose point was ~0.5-in. below the surface of the oil in the column. Precise positioning of the veil was important in providing the laminar flow that was needed to minimize coalescence of the broth droplets. The needle was normally positioned at a 35 to 45^{o} angle to the opening of the gel-forming column, with the tip of the needle positioned about 1 to 1.5 cm from the intersection of the veil and the top of the column. Silicone oil from the veil provided most of the flow through the gel-forming tube and the downstream serpentine PVC tube to the collection basket. The typical flow rate was between 200 and 300 mL/min. The other hot silicone oil stream from the pump was routed to a glass fitting at the bottom of the gelation column and flowed up through a tubular jacket that surrounded the central gelation column. The hot oil overflowed near the top edge of the gel-forming column and spilled into an overflow cup (see Fig. 2). Only a small fraction of the oil flowed into

the gel-forming column. The overflow oil flowed back to the reservoir through a PVC tube at a rate of ~150 mL/min.

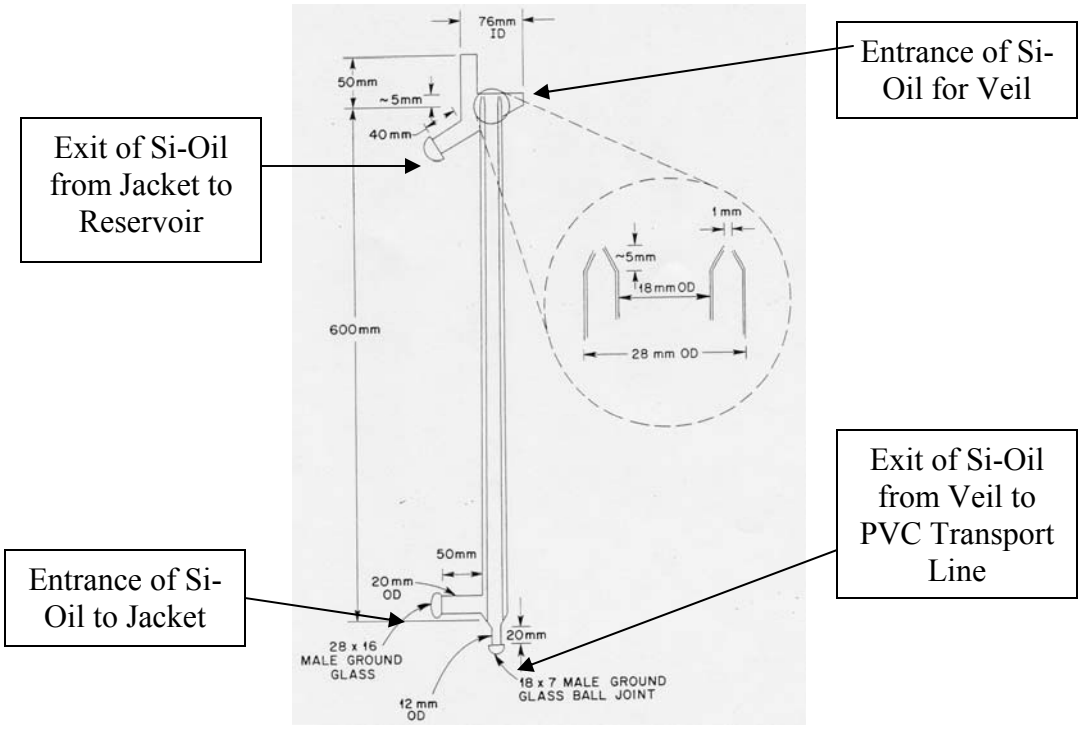

Fig. 2. Gel-forming column.

The components of the broth droplet–forming system consisted of a chilled stainless steel broth pot, a vibrator and its controller from Alpha-M Corporation (Fig. 3), a blunt-end electropolished stainless steel needle (either 19 or 21 gage) from Popper & Sons, a model 1538-A strobe light from General Radio Company, and a chilled silicone oil reservoir connected to a gear pump from Micropump, Inc. A thorough description of this system and its operation is given in Sect. 4.

3. PREPARATIONS OF ADUN STOCK SOLUTIONS FOR PRODUCTION RUNS

A stock of depleted UO_2 simulated light-water reactor pellets was used as a source of uranium for the production of kernels for the AGR Program. Preparations for producing the ADUN stock solutions that were needed to make dense kernels were developed in the 1970s and early 1980s.[17] In this task, UO_2 pellets were oxidized to a fine U_3O_8 powder in a muffle furnace in air at 600ºC (Fig. 4) to provide the starting material. In Fig. 4 the crucible on the right shows the volume of fine U_3O_8 powder that would result from the oxidation of the volume of pellets shown in the crucible on the left. The initial source of the material was the Nuclear Materials & Equipment Company

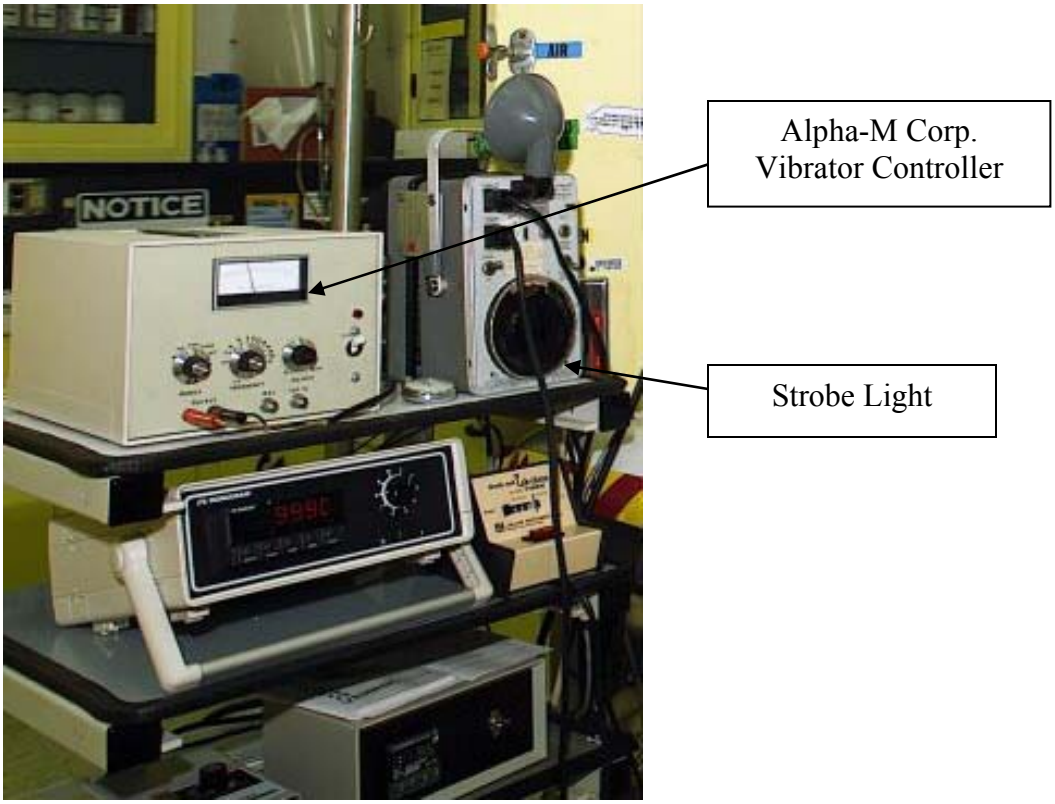

Fig. 3. Alpha-M Corporation vibrator controller and strobe light.

Fig. 4. Oxidation of UO_2 pellets to U_3O_8.

(NUMEC). The concentration range for the uranium in the ADUN stock solutions was targeted to be 2.6 to 2.9 *M,* with the NO_3^-/U mole ratio between 1.55 and 1.7. As an example, 1 L of ADUN feed was prepared by first adding ~350 mL of deionized water to 850 g of U_3O_8 powder (~50 g excess of what is needed) in a 2-L beaker on a hot plate. Next, 478 g of concentrated nitric acid was slowly added to the beaker over several hours, with occasional stirring with a Teflon stirring rod. After the first aliquot of nitric acid was added, the beaker was covered with a watch glass. The reaction is exothermic, and the formation of the reddish-brown NO_x gases is indicative of the reaction. After the final nitric acid addition, the feed solution was heated at 65ºC for several days with periodic mixing. During this period, the sample volume was increased and then maintained at approximately the 1-L mark via the addition of deionized water. Finally, the beaker was removed from the hot plate. The sample was stirred well and then equilibrated at room temperature until the excess solids had settled to the bottom of the beaker. The liquid was then removed by decantation and filtered with No. 40 filter paper into a tared 1-L plastic bottle and weighed. The density of the clear yellowish solution was measured using a clean 500-mL volumetric flask. Generally, the density was in the desired range of 1.80 to 1.85 g/mL or slightly higher. When needed, a calculated amount of deionized water was added to reduce the density to the desired range. Afterward, the density was measured again. The pH was determined using an Orion Research digital pH meter model 611 and two ROSS pH combination electrodes for accuracy. The average of the pH values was used. In most of the ADUN preparations, density and pH measurements were used to quantify the uranium concentration and the NO_3^-/U mole ratio. The relationship of molar uranium concentration to the density of uranyl nitrate solution[16] is shown in the following equation:

$$\text{Density (g/mL)} = 1.006 + 1.299 \times 10^{-3}\,[\text{U}]\ .$$

This empirical relationship is valid for uranium concentrations from 0 *M* to 2.4 *M*. To confirm these relationships, the initial uranium stock solution (UNF-8) that was prepared by this method for use in making the 350-µm-diameter kernels was subjected to several chemical analyses. The density of this solution was 1.80 g/mL, and the average pH was 1.6. Based upon the equation, the concentration was 611 g/L, or 2.57 *M*. The uranium concentration was also determined by using the Davies–Gray redox titration technique and via gravimetric analysis.[18] The Davies–Gray and gravimetric values were 626 ± 6 g/L (2.63 ± 0.03 *M*) and 628 g/L (2.64 *M*), respectively, which indicates that the density-based concentration of uranium was ~2.5% low. For all of the subsequent ADUN stock solutions, the uranium concentrations were based on 102.5% of the value calculated using the density equation.

The corrected values for uranium concentration and pH were used to determine the NO_3^-/U mole ratio, which was calculated using Fig. 3 in ORNL/TM-6850.[17] All of the prepared ADUN stock solutions in this work had NO_3^-/U mole ratios in the desired 1.55 to 1.7 range. The NO_3^-/U mole ratio for UNF-8 feed was estimated to be 1.6 using the above method. When determined by ion chromatography, the NO_3^- concentration for the UNF-8 feed was found to be 278 ± 28 g/L (4.48 ± 0.45 *M*), indicating that the NO_3^-/U mole ratio was 1.7 ± 0.17. Therefore, the calculated values from the earlier work were accurate enough.

Finally, the initial UNF-8 solution was analyzed for impurities using inductively coupled plasma–mass spectroscopy (ICP-MS) and found to be highly pure. The ICP-MS analysis revealed that the stock solution was free of other cation contaminants and contained no chloride. The only cations reported that were above the detection limit were as follows: 41.5 ± 4.2 μg/mL Ca, 6.27 ± 1.3 μg/mL Ni, 5.95 ± 0.6 μg/mL Cr, 5.19 ± 0.5 μg/mL Fe, 2.67 ± 0.3 μg/mL Mg, and 1.38 ± 0.1 μg/mL Mn. All of the analytical results showed that the uranium stock solution had the necessary purity for kernel production.

4. BROTH FORMULATION REQUIREMENTS

The preparation of high quality UO_2 kernels that were usable for TRISO coating studies required that the broth chemistry and operating parameters for making hydrous uranium oxide gel spheres be optimized. When prepared under optimum conditions, gel spheres yield kernels that are strong and near theoretical density, with excellent sphericity, minimal surface roughness, and no cracking. The initial runs conducted in the former Advanced Accelerator Application (AAA) Program to make gel sphere that yielded 300-μm-diameter UO_2 kernels had the following broth constituents: 1.14 *M* U, 1.41 *M* HMTA, 1.41 *M* urea, and 1.78 to 1.95 *M* NO_3^-. The slow-pour densities of these air-dried beads were <1.05 g/mL, and the surface quality was not as ideal as needed in this work. Furthermore, the gel spheres in the forming column had a tendency to stick together and clump and also to stick to the downstream tubing. Span-80, which is a sorbitan monooleate ester and a surface-active compound, was added to the immiscible organic medium TCE to minimize the problem encountered in earlier work. Although Span-80 is soluble in TCE, it is insoluble in silicone oil, the organic medium used in the present work. However, the clumping and sticking problem was minimized by using a more concentrated broth. The concentrations of the constituents in the optimized broth for making kernels at 60°C are shown in Table 2. When introduced into the hot silicone oil, the chilled broth droplets started to gel in 3 to 4 s for the gel spheres prepared to make 350-μm-diameter UO_2 kernels and in 4 to 5 s for the ones prepared to make 500-μm-diameter UO_2 kernels. As was previously mentioned, it was important that optimum process parameters produce air-dried $UO_3 \cdot 2H_2O$ that has a tap density in the range of 1.09 to 1.20 g/mL. It was also important that the individual kernels have an average crush strength of ≥1000 g.

Table 2. Composition of optimized broth

Constituent	Concentration (*M*)
Uranium	1.29 to 1.30
HMTA	1.68
Urea	1.68
NO_3^-	2.00 to 2.08

The uranium gel spheres shown in Figs. 5 and 6 were prepared at 60°C using the composition shown in Table 2. The diameters of the broth droplets ranged from ~1575 to 1600 μm. After washing with 0.5 *M* NH_4OH and air-drying, the yellow spheres shrank to a diameter of ~1000 μm (Fig. 5). When the spheres were calcined and sintered in a flowing stream of 4% H_2/96% Ar at 1550°C, they shrank to a diameter of ~500 μm, with an average slow-pour density of 6.68 and an average kernel density of 10.78 g/mL (see Fig. 6). The diameter shrink factor from wet gel sphere to kernel was about 3.16 ± 0.2. About 2 kg of the 500-μm kernels were prepared for the AGR coating effort. The same broth formulation and gel-forming conditions were used to make gel spheres that were sintered to 350-μm-diameter UO_2 kernels. About 4 kg of kernels were prepared.

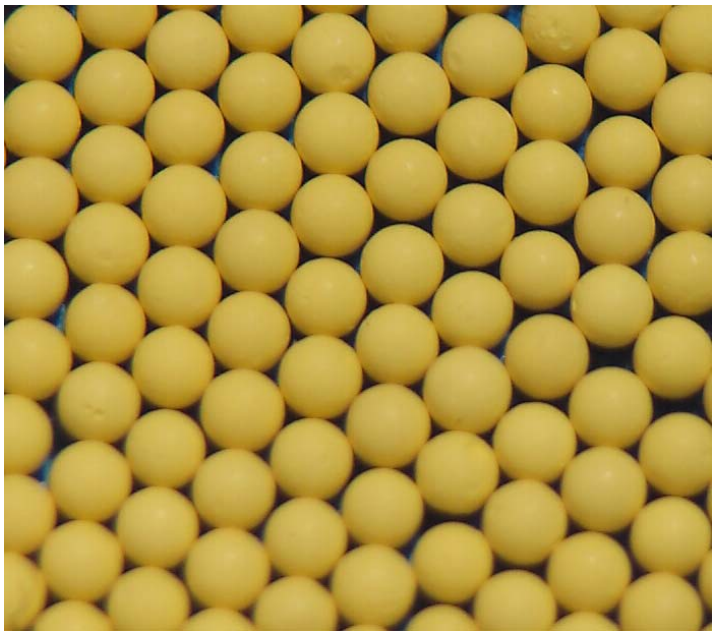

Fig. 5. Air-dried $UO_3 \cdot 2H_2O$ spheres of ~1000-μm diameter.

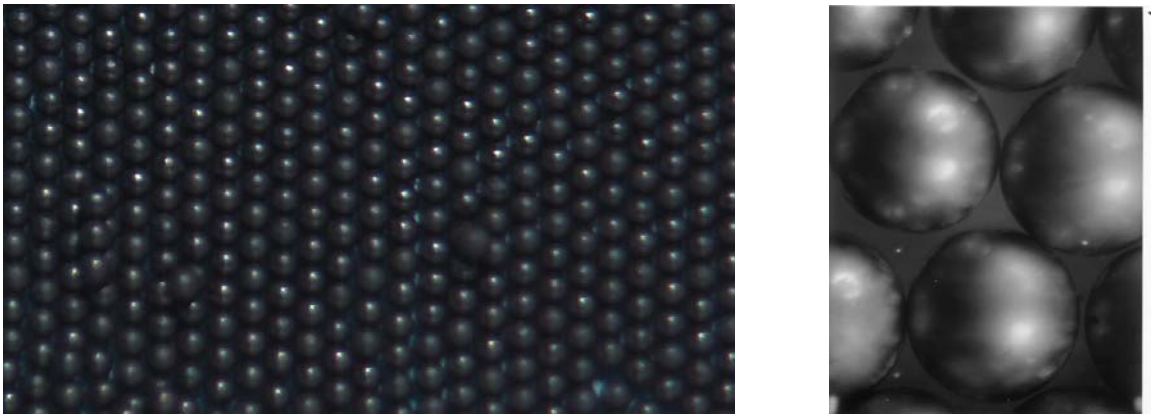

Fig. 6. Calcined and sintered 500-to 532-μm-diameter UO_2 kernels, with the further magnified kernels on the right showing the sphericity and surface quality.

5. BROTH DROPLET–FORMING SYSTEM AND OPERATION

For preparation of gel spheres that yielded sintered UO_2 kernels with a diameter of ~500 μm, the broth droplet–forming system consisted of the following components: a chilled stainless steel broth pot, a vibrator and its controller from Alpha-M Corporation, a blunt-end electropolished stainless steel needle (19 gage) from Popper & Sons, a model 1538-A stroboscopic light from General Radio Company, and a chilled silicone oil reservoir connected to a gear pump from Micropump, Inc. (see Fig. 7). About 211 mL of chilled broth was first added to the broth pot. Afterward, the chilled silicone oil was pumped via the gear pump at a rate of 15 mL/min into an inlet tube located on top of the sealed broth pot. The immiscible oil, which has a lower density than the broth, floated on top of the broth and forced the chilled broth out an outlet tube located at the bottom of the pot into a 3/16-in.-ID PVC tube that was ~3-ft long. The other end of this tube was connected to a glass observation tube, which had a male Luer fitting for attaching the needle. For best results during a run, the needle was positioned at a 35 to 45° angle (Fig. 8) to the veil of hot silicone oil. The jet stream of droplets was aimed toward the bottom of the veil from ~2 to 5 mm above the top of the gel-forming column. The tube passed through the vibrator, which was positioned ~30 to 45 cm from the needle. The goal was to produce uniform droplets that were ~1600 μm in diameter. To do so, the controller was set to provide a frequency of 128 Hz/s at an amplitude of ~1.5, which equates

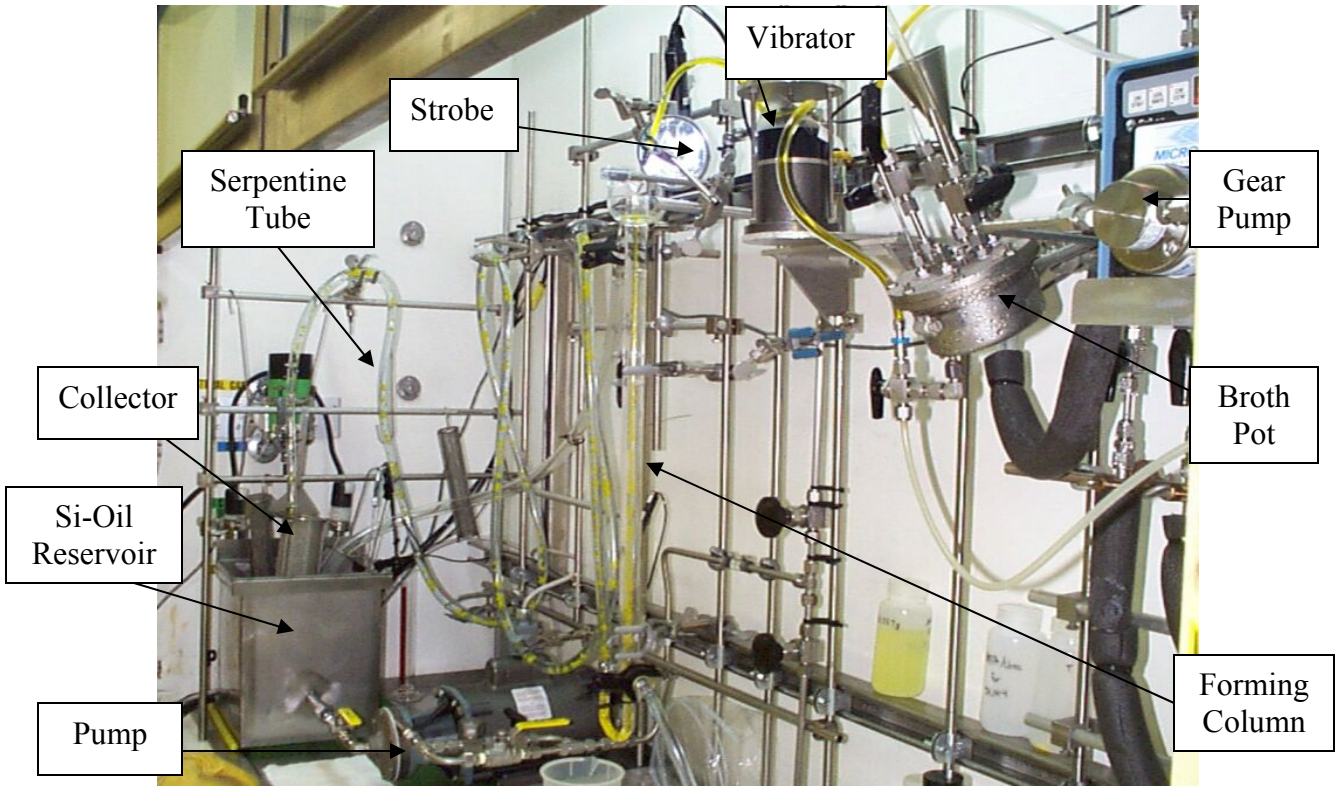

Fig. 7. Laboratory-scale apparatus for converting chilled broth into uniform gel spheres.

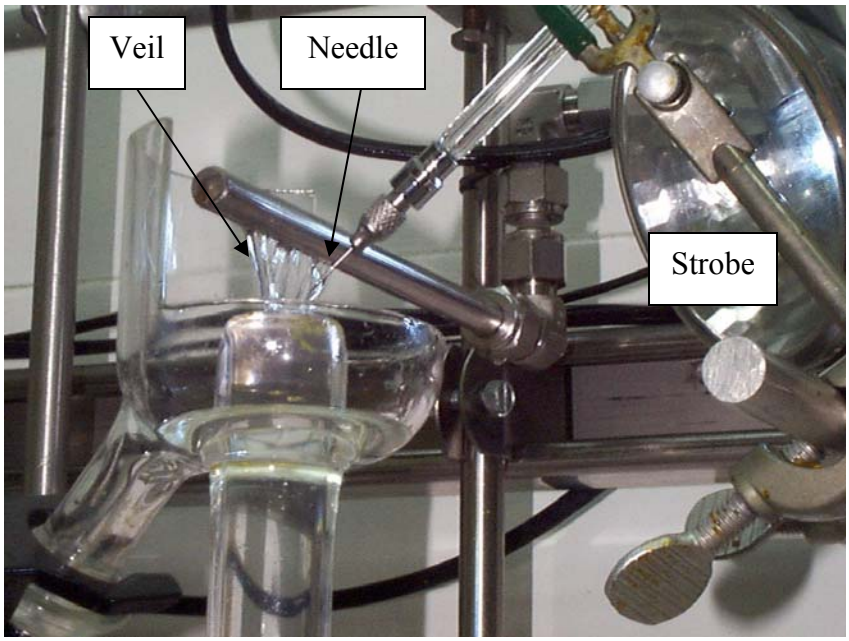

Fig. 8. Ideal positioning of blunt-end needle relative to the veil of silicone oil.

to 7680 cycles/min or droplets/min. The stroboscopic light was set at ¼ (7680) or 1792 to provide more apparent visible distance between the droplets (see Sect. 6 for details). The key was to fine-tune the amplitude so that the stream of droplets appeared to be stationary with no blurring or flickering when observed with the stroboscopic light.

At the beginning of the campaign to prepare 3.5 kg of sintered UO_2 kernels that were 350 ± 10 μm in diameter, the controller manufactured by the Corporation Alpha-M began to malfunction and became difficult to control. Because the Alpha-M Corporation went out of business several years ago, it was impossible to obtain a new controller or replacement parts to repair the old one. Fortunately, the ORNL Nuclear Science and Technology Division provided funding for the purchase of a new automatic controller and vibrator from Labworks, Inc. The system consisted of an ET-132-2 electrodynamic shaker (Fig. 9) with an SC-121 sine servo controller system (see Fig. 10). A low-impedance accelerometer from Kistler Instrument Corporation was also purchased as part of this system. Figure 11 shows the accelerometer attached to the armature of the shaker and positioned underneath the PVC tubing. A micro coax connector cable is connected from the side of the accelerometer to the sine servo controller. Operation in servo mode provided constant acceleration of the vibrator. Using acceleration feedback, the servo continuously adjusts its output signal amplitude to that required by the vibrator. Once the system was put into operation and optimized, it proved to be a much better frequency controller for preparing gel spheres than the manually controlled Alpha-M Corporation control system and proved to be very effective in providing high yields of UO_2 kernels in the targeted 350±10-μm-diameter range. The operation of this vibratory system was very different from the Alpha-M Corporation system used previously. The use of an accelerometer in connection with the sine servo controller provided automatic control of

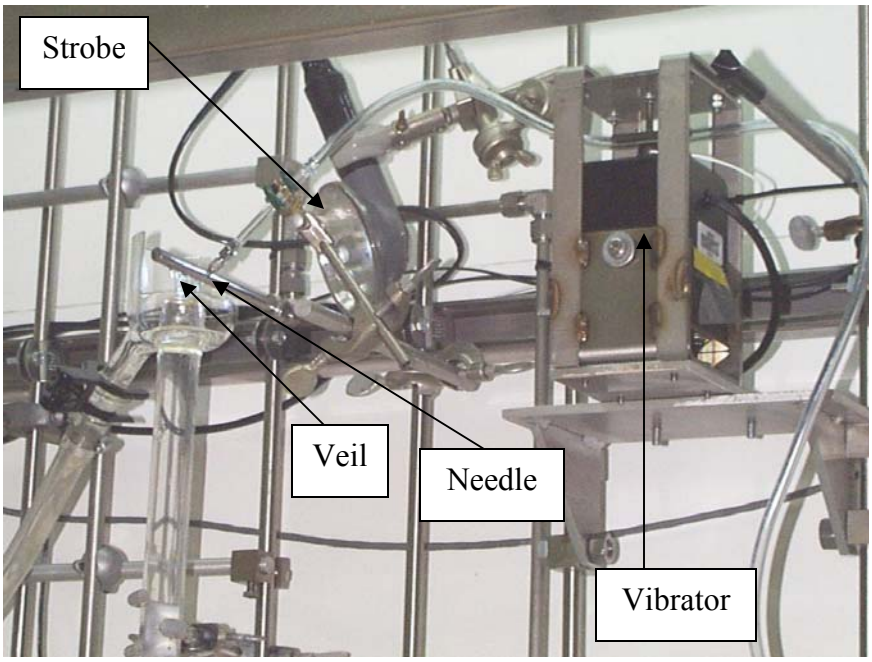

Fig. 9. Electrodynamic shaker.

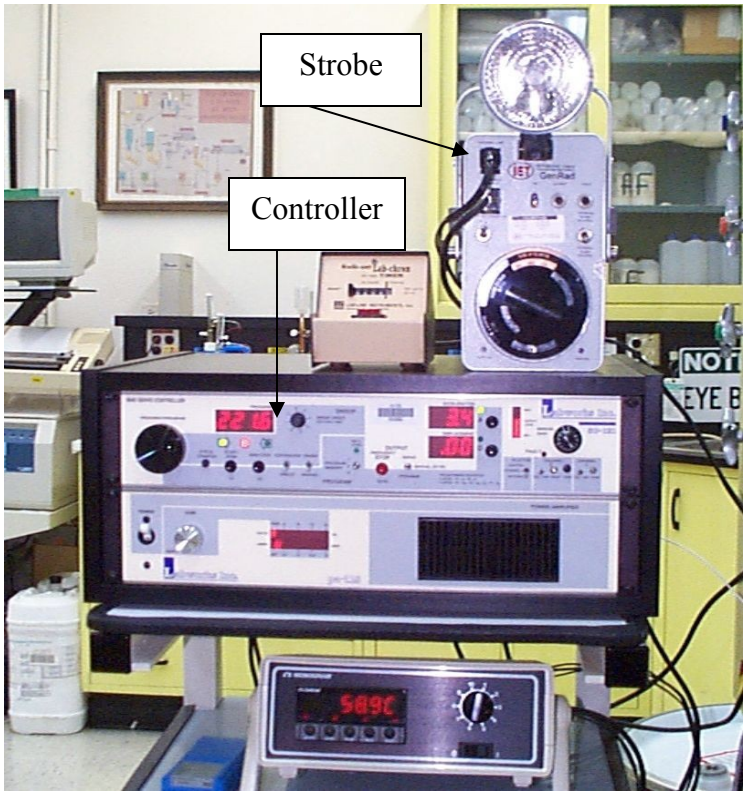

Fig. 10. Sine servo controller system and strobe light.

Fig. 11. Low-impedance accelerometer positioned underneath tube.

the frequency. When the frequency was set correctly, very uniform broth droplets of the targeted size were delivered from the needle as a jet stream to the forming column. The optimum settings used to make the 350±10-µm kernels were as follow: 221 cycles/s for the frequency, an output level of 60 to 70%, an acceleration reading of 3 to 4 for the sine servo controller, and 1 V and 1 to 2 A at full gain for the power amplifier. The key was to keep the output level in the 60% to low 70% range The stroboscopic light was set at ¼ [(221 cycles/s)(60 s/min)], or 13,260 cycles/min. The frequency was confirmed with the stroboscopic light.

Custom-designed stainless steel needles were purchased from Popper & Sons. The specifications are shown in Fig. 12. The key to the design was to have a circular, burr- and crack-free, tapered blunt-end orifice that had been mildly electropolished. The new vibrating system and needle have produced outstanding results and have made it possible for the production runs to have very high yields of targeted kernels, with no satellite side streams. For example, 97.5% (347.7 g) of the air-dried spheres that were obtained from runs DUN-176 through -179 were in the targeted 600- to 850-µm-diameter sieve fractions and had an average slow-pour density of 1.08 g/mL. Calcining and sintering of the spheres produced 286.4 g of UO_2 kernels, which were then sieved with precision sieves. The weight loss was 17.5%, and the slow-pour density was 6.7 g/mL. The sieving results were as follows: 0.1 g (<322 µm), 0.6 g (332–342 µm), 269.7 g (342–359 µm), 12.6 g (359–368 µm), 2.2 g (368–425 µm), and 1.2 g (>425 µm). About 94% of the sintered kernels were in the 342–359-µm fraction (or 350 ± 8 µm), and 98.6% were in the 332–368-µm fraction (or 350 ± 18 µm). The slow-pour density of a sample of the

342–359-µm fraction was 6.7 g/mL. More detailed information about the results is provided in Sect. 8 of this report.

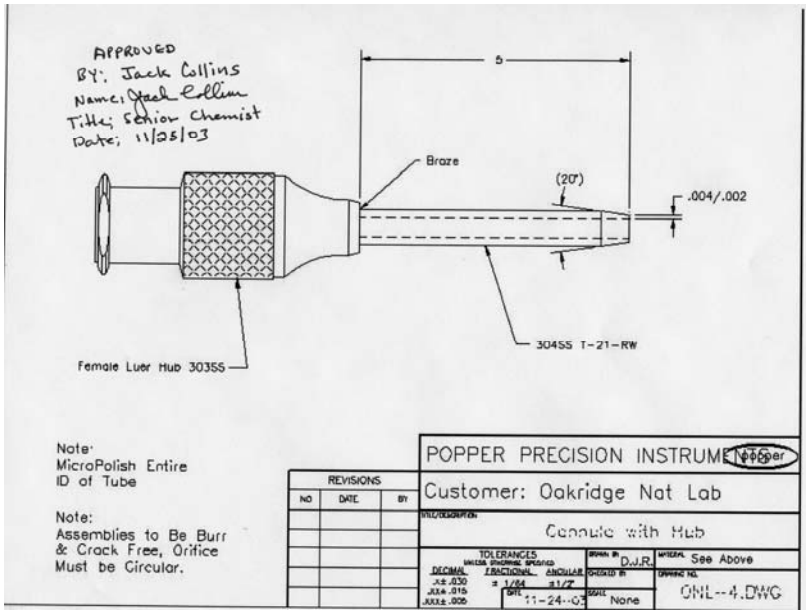

Fig. 12. Custom-designed stainless steel needle made by Popper & Sons for the 350 ± 10-µm kernels.

An undesirable problem was encountered early in the production runs using the new vibrating system, in which spheres of two different sizes were predominately produced. For example, the sieved air-dried fractions for run DUN-120, which was conducted on December 17, 2003, were as follows: 0.7 g (>1400 µm), 3.0 g (1180 to 1400 µm), 5.2 g (1000 to 1180 µm), 22.2 g (850 to 1000 µm), 12.2 g (710 to 850 µm), 39.4 g (600 to 710 µm), 0.0 g (500 to 600 µm), 0.0 g (425 to 500 µm), and 0.2 g (<420 µm). This type of bimodal problem occurred with the first seven runs. Afterward, six good-to-excellent runs were made. The bimodal problem then returned intermittently for the next 19 runs, a phenomenon that was difficult to understand. Although the problem was initially thought to be in the controller, this did not prove to be the case. Fortuitously, it was discovered that the top surface of the accelerometer had to be perfectly positioned parallel with the plastic tube and the split stainless steel tube above it (Fig. 11). Runs (e.g., DUN-120) that were bimodal were the result of the accelerometer being tilted with respect to the plastic tube, a small misalignment that was very difficult to see. After this discovery (starting with run DUN-149), the accelerometer was pressed down several times with a screwdriver to position it correctly. Any subsequent repositioning of the plastic tube required that the accelerometer be repositioned in a similar manner. The armature of the old Alpha-M vibrator was very rigid, and the importance of the lateral play of the armature of the new vibrator was not initially recognized as being critical to uniform drop formation. Figure 13 compares data from three ideal runs (DUN-183, -179, and -137) with those from three of the bimodal runs

(DUN-131, -130, and -120). For these bimodal runs, the bulk of the mass of the kernels were in the 600–710-µm and 850–1000-µm fractions, with the mass of the 710–1000-µm fraction being much less. In reviewing the run sheets of 86 runs in which the new vibrating system was used, 16 were identified as severely bimodal and 4 as slightly bimodal. The sizes of the bimodal fractions were probably dependent upon the degree of tilt of the accelerometer. Once the problem was recognized and corrected, no bimodal runs occurred during the last 34 runs of the campaign.

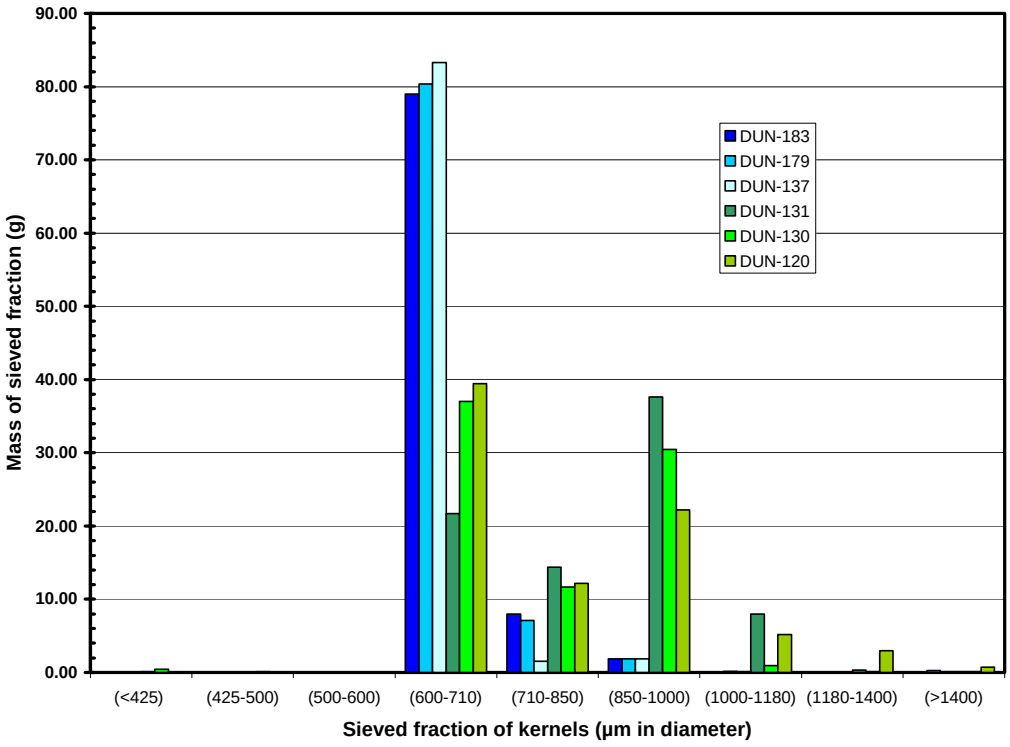

Fig. 13. Comparison of sieve data from three ideal runs with those from three bimodal runs.

Several other droplet-control problems that can occur during a run required care and vigilance before and during the run. It was important that the broth vessel, glass observation tube, stainless steel needle, and plastic tubing used between the broth vessel and the needle be thoroughly cleaned before starting a new run. Generally, a new section of plastic tubing was used for each run. Any gelled broth deposits not removed during cleaning from the previous run could dislodge, transport to, and plug the needle. Also, after the pumping of chilled silicone oil to the broth vessel was started, it was important to degas the outlet tube and valve of the broth vessel. This step reduces the possibility of air bubbles being transported to the section of plastic tubing between the vibrator and the needle, an area in which a trapped bubble can cause nonuniform drop formation. The vibration of the broth jet stream as it exits the needle is caused by the pulses on the broth flowing through the plastic tube by the vibrator (Fig. 11). An air bubble, especially if it is large enough to occupy the full diameter of the plastic tube, can disrupt the transmission of the pulse to the needle and dampen the vibration of the jet stream.

6. CALCULATIONS TO DETERMINE NEEDLE SIZES AND VIBRATOR FREQUENCIES FOR KERNEL PREPARATION

The following discussion is based on information contained in a journal article published by P. A. Haas in the early 1990s.[13] Hass describes how a liquid jet discharged from a small opening under laminar flow conditions tends to break into short lengths, which then form spherical drops. This behavior results from surface energy or interfacial tension. The most probable jet length between break points is about 5 times the diameter of the jet stream, a length that gives a spherical drop diameter about twice that of the jet diameter. A controlled and uniform vibration can be applied to a liquid jet to produce the disturbances that control jet breakup. If the frequency of the vibration is near the natural frequency for laminar breakup, there will be good control of the breakup and drops formed will be very uniform in size.

In Haas's work, only a single needle (called a "single-fluid nozzle") was used. For a jet with a diameter of d and a velocity of v (in centimeters per second), the natural frequency of drop formation is near $v/5d$. It is assumed that the jet diameter and the inside diameter of the needle orifice are equal, although they can be slightly different. From the volume balance, the drop diameter (D) for the natural frequency of drop formation is $1.96d$. The distance between drops is then $5d - 1.96d$, or about $1.5D$. In practice, vibration at 0.666 to 1.5 times the natural frequency, which forms drops of ±14% of the natural drop diameter, will generally allow excellent formation control.[13] Useful results can be obtained at 0.5 to 2 times the natural frequency ($2.46d > D > 1.55d$). Better results are obtained by changing the orifice or jet diameter in order to achieve conditions that more closely match those for natural breakup. The jet diameter should be about one-half the intended drop diameter. Empirical results showed that the best values for D/d range from ~2.05 for 600-µm drops to 2.3 for 5000-µm drops.

To be able to form broth droplets that yield 350±10-µm-diameter sintered UO_2 kernels, it was important to know to what extent the diameter of the broth droplets or gel spheres would shrink. The shrinkage was calculated by the following equation:

$$D/D_p = \text{diameter shrinkage} = \left[\frac{\text{UO}_2 \text{ kernel U concentration}}{\text{broth U concentration}}\right]^{0.333} .$$

The following sample calculation is for broth droplets with a uranium concentration of 1.30 M which, after being air-dried, calcined, and sintered, shrink to form UO_2 kernels with a density of 10.96 g/mL. Broth droplets with this concentration have a shrink factor of 3.145:

$$D/D_p = \left[\frac{(10.96)(1000)/270}{1.30}\right]^{0.333} = 3.145 .$$

Figure 14 is a plot of the gel-sphere shrink factor as a function of the uranium concentration of broth droplets for the production of UO_2 kernels with a density of 10.96 g/mL. Note that the shrink factor increases from 3.145 for 1.3 M uranium to 3.325

for 1.10 *M* uranium. To prepare UO_2 kernels with diameters of 350 or 500 μm, the broth droplets with a concentration of 1.30 *M* uranium would need to be 1100 or 1572 μm, respectively. For the case in which the concentration is 1.10 *M* uranium, the droplet diameters would need to be 1164 or 1663 μm, respectively, for kernel diameters of 350 and 500 μm.

For the 350-μm-diameter kernel runs, a stainless steel needle with an approximate orifice diameter of ~500 μm or (1100/2.2) was needed. A 21-gage needle, which has an inside diameter of 510 μm, was chosen because of its closeness to ideal (see Fig. 12). The orifice diameters for 22- and 20-gage needles are 410 and 580 μm, respectively.

Before calculations were made to determine the frequencies needed to make 1100- and 1572-μm-diameter broth droplets, the ideal laminar jet flows for these nozzles had to be determined. The ideal flow rate for each needle was determined empirically by pumping water through the needle, which was positioned at a 40^o angle with respect to the top of the column. The jet stream was observed using the stroboscopic light, and the plastic tube was pulsed with the vibrator at a distance of about 40 cm from the needle. The trick was to adjust the flow rate while observing the outflow of broth droplets from the needle. Dripping occurred when the jet velocity was too slow. A flow rate was chosen in which the jet velocity was on the low side of being optimum but well within the preferred zone (shown in Fig. 15). The flow rates decided upon for the 21- and 19-gage

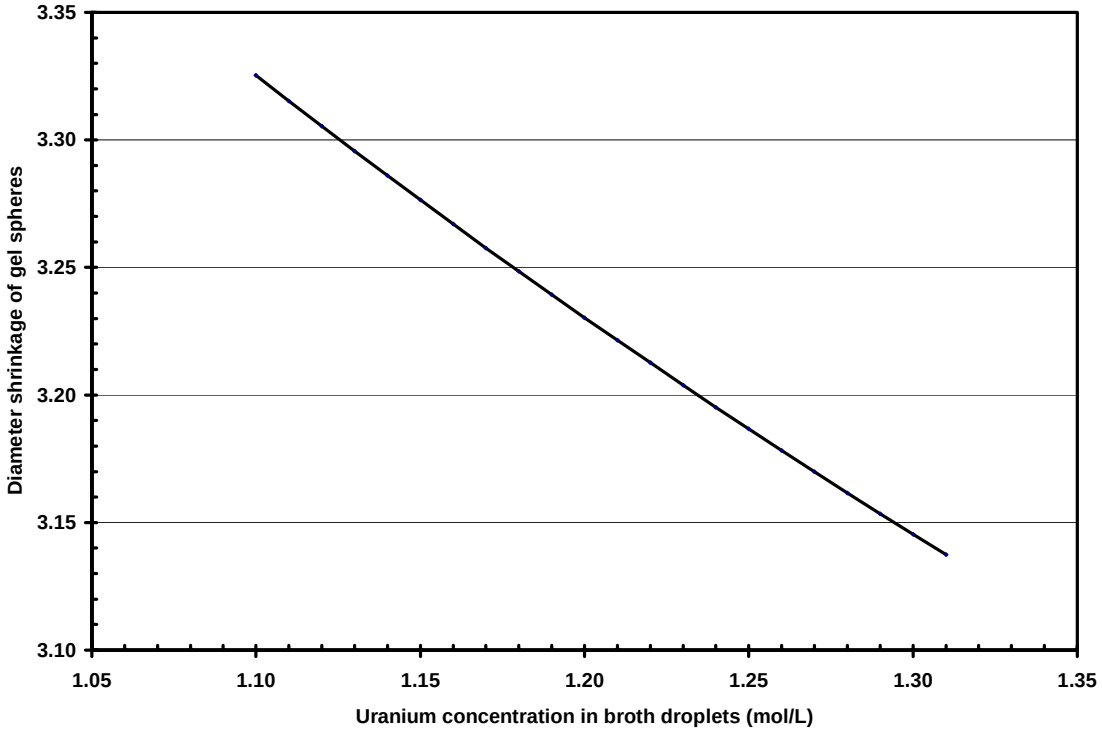

Fig. 14. Shrinkage of gel spheres as a function of uranium concentration in the broth to produce UO_2 fuel kernels of theoretical density.

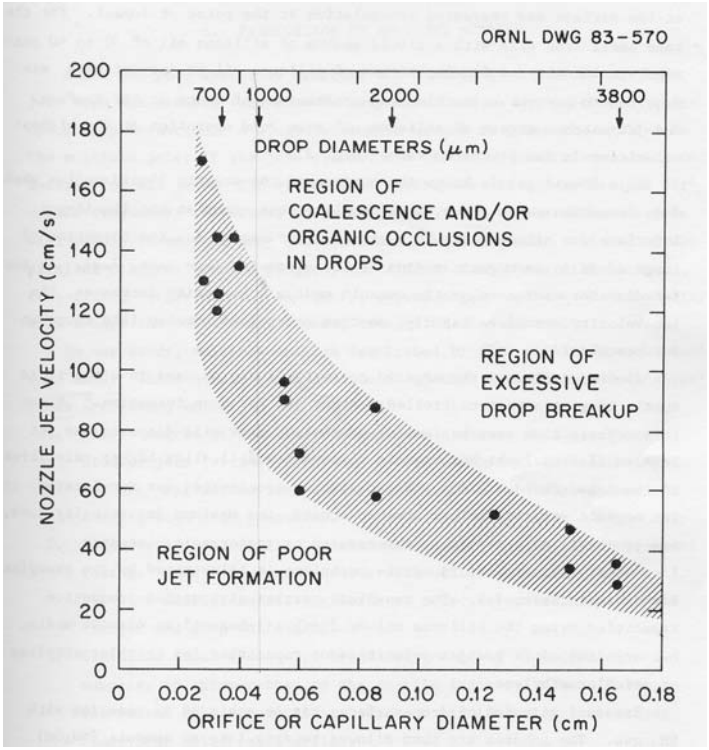

Fig. 15. Preferred jet velocities for single-fluid nozzles.

needles were 9.3 mL/min (0.155 cm^3/s) and 15 mL/min (0.250 cm^3/s), respectively. The jet velocity for the 21-gage needle is calculated as follows:

$$\text{Jet velocity} = \text{Flow rate/Area of needle orifice}$$
$$= \frac{(0.155)}{(3.1416)[(0.051/2)]^2} = 76 \text{ cm/s} ,$$

which gives uniform drop formation for 1100-µm-diameter drops. To make the 500-µm kernels with a 19-gage needle with a 680-µm-diameter orifice and a flow rate of 0.250 cm^3/s, the jet velocity was calculated to be 69 cm/s, which is also within the ideal zone needed to make uniform 1572-µm-diameter drops.

For a typical volume of broth of 210 cm^3 used in a run, ~301,680 drops with a diameter of 1100 µm could potentially be made. This is determined by first calculating the drop volume and then dividing the broth volume by the drop volume:

$$\text{Volume of a 1100-µm-diameter drop} = 4/3\pi r^3 = 0.0006961 \text{ cm}^3 ,$$

and

$$\text{Number of possible droplets} = 210 \text{ cm}^3/0.0006961 \text{ cm}^3/\text{drop} = 301{,}680 .$$

The frequency is calculated as follows for the case of a 21-gage needle and a broth flow rate of 9.3 cm^3/min (0.155 cm^3/s):

Frequency = (number of drops formed)/s = flow/drop volume

= (0.155 cm^3/s)/(0.0006961 cm^3/drop) = 222.7 drops/s .

This means that the top of the accelerometer of the vibrator would need to press the plastic broth tube ~223 times per second or 13,380 times per minute.

For the case of a 19-gage needle and a flow rate of 15 cm^3/min (0.25 cm^3/s), the frequency needed to make 1572-µm-diameter droplets is 123 drops/s, or (0.250 cm^3/s)/(0.002034 cm^3/drop). The number of broth drops that can potentially be prepared with the same 210 cm^3 of broth is only 103,245.

7. CALCINATION AND SINTERING OF $UO_3 \cdot 2H_2O$ TO PRODUCE UO_2 KERNELS

Before beginning the process of calcining and sintering the air-dried $UO_3 \cdot 2H_2O$ spheres used in this program, a few samples of microspheres were analyzed by differential thermal analysis (DTA) and thermogravimetric analysis (TGA) to gain a better insight into the volatility and decomposition behavior of the residual HMTA, urea, and NH_4NO_3 remaining in the spheres. If these contaminants decompose too rapidly, internal gas pressures can crack the microspheres. Furthermore, if the microspheres are heated too rapidly at temperatures in the range of 50 to 150ºC, steam pressure from the free water and water of hydration can also cause the microspheres to crack. TGA profiles represented as percent weight loss as a function of temperature in a 100% N_2 atmosphere are shown in Fig. 16 for samples of pure HMTA, NH_4NO_3, and urea that were separately heated and measured. The rapid weight loss for the HMTA, urea, and NH_4NO_3 samples began at 130, 140, and 180ºC, respectively. Most of the HMTA, NH_4NO_3, and urea had disappeared by the time the temperatures reached 240, 280, and 370ºC, respectively.

DTA and TGA profiles were also obtained for heating a sample of 750-µm-diameter air-dried $UO_3 \cdot 2H_2O$ microspheres to 1000°C in a 4% H_2/96% Ar atmosphere, as shown in Fig. 17. The TGA profile showed that the microspheres continued to lose weight until the temperature reached 590ºC. Afterward, the TGA profile remained fairly constant. The microspheres lost about 6.9% of their total mass at temperatures below 150ºC. Most of this weight loss was probably due to the loss of water. At least part of the weight loss between 120 and 370°C would be attributed to HMTA, urea, and NH_4NO_3 contaminants. No weight loss for these contaminants would be expected above 350ºC; any subsequent weight loss at higher temperatures was probably due to the conversion of UO_3 to U_3O_8 and then to UO_2. By the time the temperature reached 590ºC, the conversion was complete. The weight loss for the sample was 22.3%. In the production runs, the typical weight loss as a result of calcining and sintering was about 17.5%.

Based upon TGA and DTA data, a calcining and sintering profile shown in Fig. 18 was developed and used in the campaigns to successfully convert the $UO_3 \cdot 2H_2O$

microspheres to near theoretically dense UO_2 kernels with no evidence of cracking. The air-dried microspheres were first heated in a flowing 4% H_2 /96% Ar atmosphere for 2 h at 80ºC to permit free water to escape. The spheres were then heated for 3 h at 150ºC to slowly remove the HMTA, urea, and NH_4NO_3 contaminants; then heated for 5 h at 600ºC to convert the UO_3 to U_3O_8 to UO_2; and finally heated for 5 h at 1550ºC to densify the UO_2 kernels. The flow rate of the 4% H_2/96% Ar was ~3 L/min.

The tube furnace and controller (shown in Fig. 19), were purchased, installed, and became operational on August 12, 2003. The furnace used a 4-in.-diameter alumina tube with stainless steel end caps, which were custom designed and fabricated. The end caps included O-ring seals and were water cooled to ensure that the O-ring temperature was maintained below the maximum operating temperature of 280°C.

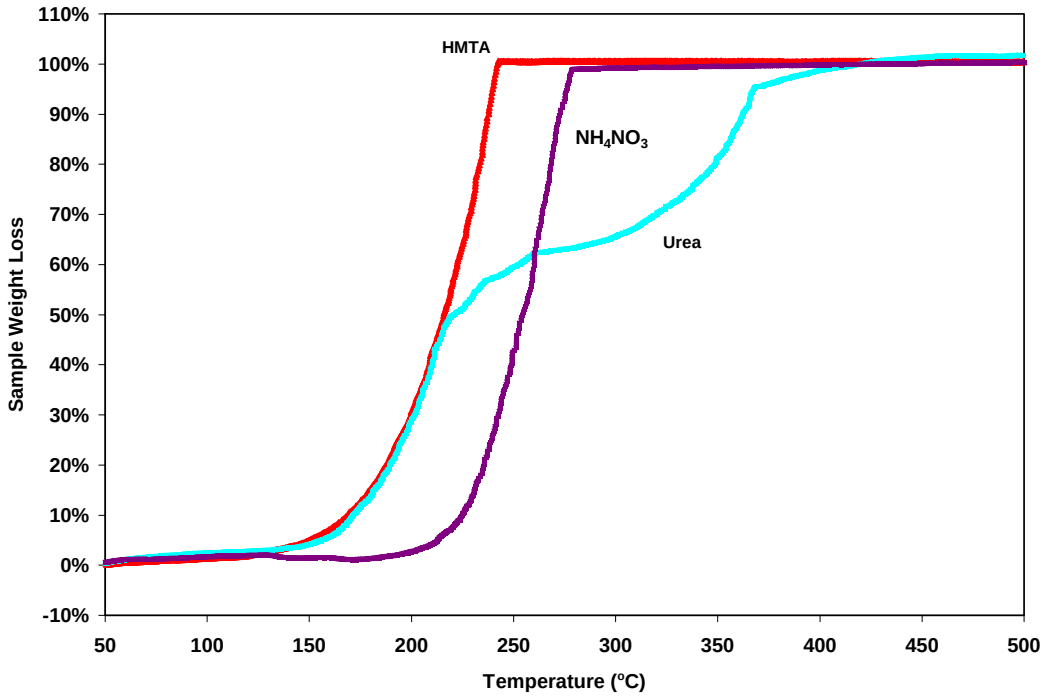

Fig. 16. TGA weight-loss profiles for samples of pure HMTA, NH_4NO_3, and urea in a 100% N_2 atmosphere.

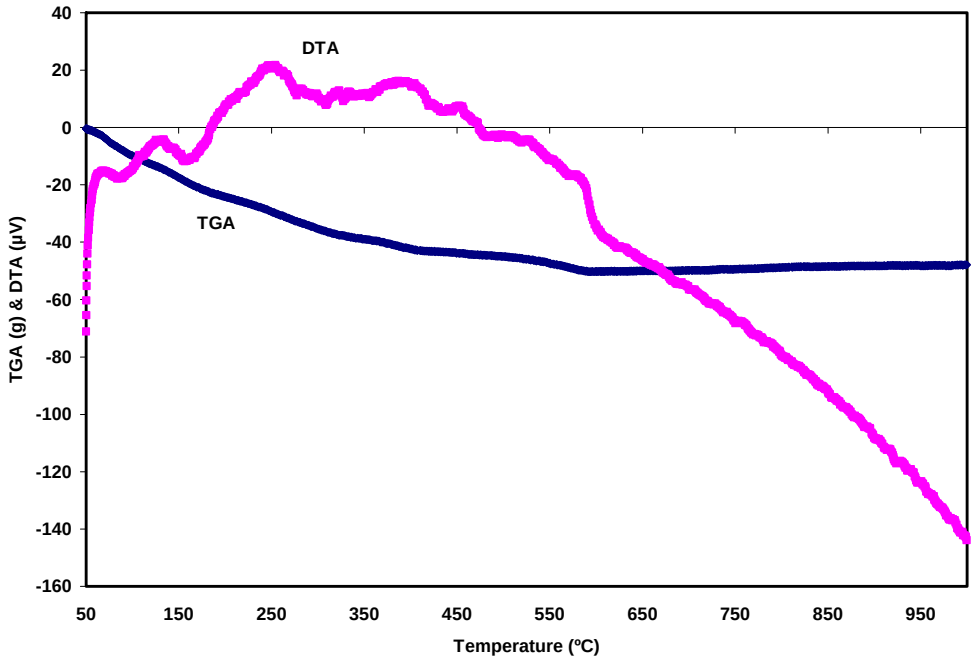

Fig. 17. TGA and DTA profiles for heating 750-µm-diameter air-dried $UO_3 \cdot 2H_2O$ microspheres to 1000°C in a 4% H_2/96% Ar atmosphere.

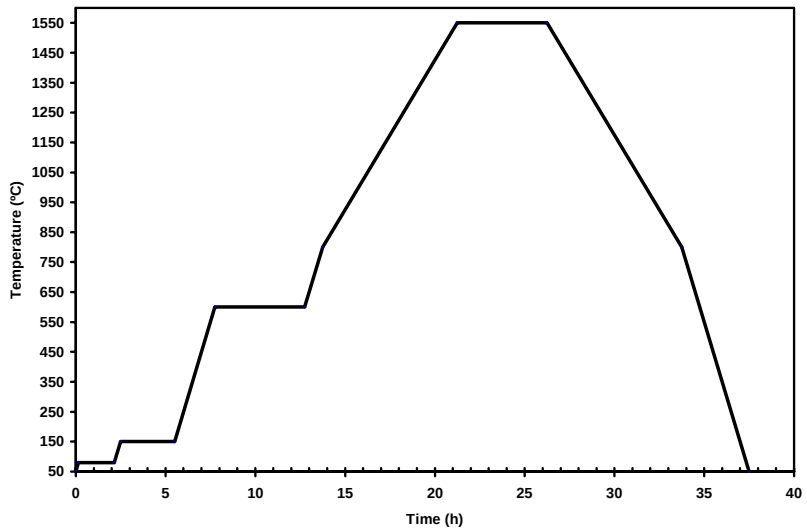

Fig. 18. Typical calcining and sintering heating profile for the UO_2 kernels.

Fig. 19. Tube furnace and controller used for calcining and sintering air-dried spheres.

8. PRODUCTION CAMPAIGN TO PRODUCE 2 kg OF 500±20-µm-diameter UO_2 KERNELS

The initial task of the AGR kernel production effort was to produce 2 kg of 500±20-µm-diameter UO_2 kernels. To accomplish this goal, 45 gel sphere–forming runs were made between March 3 and May 27, 2003. The sieving results obtained in these runs for the air-dried $UO_3 \cdot 2H_2O$ microspheres are summarized in Table 3; the slow-pour densities of samples of microspheres are also given. During the time that these runs were made, there was no capability to calcine and sinter the product to obtain sintered and densified kernels. The production effort was based upon best kernel production information obtained from earlier work at ORNL. The goal was to produce wet gel spheres with a diameter of about 1572 µm. Upon being air-dried, these spheres shrank to a diameter near 1000 µm. Based upon this targeted diameter, the two fractions of spheres between 850 and <1180 µm in diameter were combined and held for calcining and sintering. A total of 3.33 kg of targeted spheres were produced, or 86% of the total production yield. The slow-pour density was in the desired range of 1.1 to 1.2 g/mL, with the average being ~1.17 g/mL. The average crush strength was in the 500- to 600-g range.

Three batches of calcined kernels were sintered in the tube furnace (Fig. 19) in a flowing stream of 4% H_2/96% Ar at 1550ºC to produce 2452 g of product. The batches were sieved with Budkbee-Mears precision sieves. The sieving data are summarized in Table 4. Of these kernels, 2016 g were in the 482- to 532-µm-diameter range, or 82.2% of those produced. The usable UO_2 kernel product represents 71% of possible UO_2 kernels from the broth droplets for the 45 runs.

Table 3. Sieve fractions and slow-pour densities of air-dried microspheres produced in the campaign to make 500-µm-diameter kernels with the Alpha-M Corporation controller and vibrator

		Mass of sieve fraction (g)								
Run no.	Total mass of dried spheres (g)	>1180 µm	1000–1180 µm	850–1000 µm	710–850 µm	600–710 µm	500–600 µm	420–500 µm	<420 µm	Slow-pour density (g/mL)
DUN-43	85.05	1.30	0.97	81.83	0.25	0.04	0.36	0.27	0.03	1.15
DUN-44	85.90	2.13	1.39	81.72	0.25	0.04	0.17	0.15	0.05	1.15
DUN-45	85.68	29.31	7.38	47.48	0.45	0.13	0.45	0.39	0.09	1.21
DUN-46	85.79	0.81	3.37	77.13	0.57	0.42	0.84	2.06	0.59	1.21
DUN-47	84.98	18.21	6.74	49.13	0.61	0.48	8.59	0.84	0.38	1.20
DUN-48	86.10	0.39	0.31	75.46	0.57	0.03	2.90	5.14	0.39	1.19
DUN-50	83.04	4.86	3.7	71.85	0.55	0.09	1.14	0.76	0.09	1.18
DUN-51	88.16	0.69	1.67	79.02	1.88	0.08	2.73	1.85	0.24	1.21
DUN-52	86.30	2.53	5.15	76.85	0.23	0.10	1.05	0.36	0.03	1.19
DUN-53	63.47	10.61	16.23	32.99	0.16	1.04	2.32	0.09	0.03	1.14
DUN-54	108.00	14.14	38.24	46.72	0.14	1.59	5.67	1.31	0.19	1.16
DUN-55	86.34	5.89	40.01	31.35	0.20	0.72	3.62	4.23	0.32	1.17
DUN-56	87.66	10.3	43.37	27.46	0.01	0.19	1.75	4.43	0.15	1.17
DUN-57	85.65	7.89	41.74	32.68	0.06	0.11	0.79	2.31	0.07	1.15
DUN-58	85.50	9.64	26.91	42.84	0.05	0.17	3.86	1.88	0.15	1.15
DUN-59	87.04	3.16	15.69	56.07	0.40	1.41	7.71	1.10	1.50	1.14
DUN-60	85.70	4.15	19.30	53.37	0.09	0.10	8.51	0.13	0.05	1.15
DUN-61	88.99	8.19	22.48	49.45	0.08	0.16	6.52	1.99	0.12	1.16
DUN-62	84.08	1.67	19.39	56.95	0.04	1.90	0.82	2.65	0.66	1.15
DUN-63	83.42	2.54	40.63	36.86	0.06	0.29	0.38	1.86	0.80	1.12
DUN-64	87.86	1.84	18.18	57.73	0.15	1.84	1.63	4.85	1.64	1.15
DUN-65	86.19	3.56	22.44	53.90	0.03	0.18	4.25	1.74	0.09	1.14
DUN-66	88.13	5.58	25.38	49.58	0.01	0.16	6.14	1.19	0.09	1.15
DUN-67	87.41	0.96	29.89	50.00	0.03	0.42	5.62	0.43	0.06	1.17
DUN-68	88.06	0.74	26.34	55.99	0.07	0.13	1.51	3.27	0.01	1.16
DUN-69	84.12	5.06	9.49	63.64	0.46	1.03	1.02	1.65	1.77	1.17
DUN-70	88.39	5.76	10.56	61.66	0.03	0.07	8.98	1.23	0.10	1.17
DUN-71	88.45	0.71	21.37	57.96	0.04	0.12	6.78	0.91	0.56	1.17
DUN-72	87.12	0.40	31.89	46.54	3.52	2.26	2.04	0.09	0.38	1.16
DUN-73	84.82	0.55	24.41	55.98	0.05	0.09	1.80	1.78	0.16	1.15
DUN-74	84.96	0.49	12.06	67.98	0.05	0.13	0.50	2.97	0.78	1.17
DUN-75	81.29	1.40	22.63	56.03	0.07	0.32	0.30	0.44	0.10	1.16
DUN-76	83.94	0.59	21.70	56.38	0.31	0.13	2.75	1.97	0.11	1.15
DUN-77	82.23	28.38	12.37	34.31	2.70	2.23	1.41	0.60	0.33	1.15
DUN-78	84.76	1.95	17.37	61.00	0.14	0.37	0.16	3.34	0.43	1.16
DUN-79	83.96	3.89	10.01	64.55	1.86	1.92	0.29	0.83	0.61	1.21
DUN-80	88.06	1.72	6.23	71.63	0.83	1.56	0.60	3.63	1.86	1.19
DUN-81	80.27	4.75	18.45	54.70	0.14	0.17	1.64	0.31	0.11	1.18
DUN-82	86.94	1.26	13.51	53.49	8.38	0.66	6.31	1.90	1.43	1.17
DUN-83	82.13	3.06	11.56	62.54	0.14	0.13	0.94	2.31	1.45	1.15
DUN-84	85.44	0.57	7.03	71.69	0.20	0.79	0.53	2.92	1.71	1.17
DUN-85	88.77	0.52	13.88	66.85	0.14	0.99	0.58	3.72	2.09	1.19
DUN-86	84.98	0.45	10.32	68.31	0.26	1.26	0.53	2.50	1.35	1.19
DUN-87	82.39	4.65	10.70	62.63	0.02	0.01	3.00	1.34	0.04	1.18
DUN-88	84.53	24.39	22.72	32.19	0.20	0.08	2.56	2.31	0.08	1.16
Total	3852.1	241.64	785.16	2544.47	26.48	26.14	122.05	82.03	23.27	
		(6.27%)	(20.38%)	(66.05%)	(0.69%)	(0.68%)	(3.17%)	(2.13%)	(0.60%)	

Table 4. Summary of sieving data for the sintered 500-µm-diameter UO_2 kernels

Diameter of sieved fraction (µm)	Mass (g)
>532	259
518–532	815
500–518	929
496–500	71
482–496	201
<482	177
Total	2452

Two separate batches of kernels were prepared. One batch was prepared by removing 114 g of kernels from the 500- to 518-µm-diameter fraction and combining it with the 496- to 500-µm- and the 482- to 496-µm-diameter fractions for a total weight of 386 g in the 482- to 518-µm-diameter range. The batch was then thoroughly blended with a Jones riffle splitter (Fig. 20) and sorted into three 100-g samples and one 86-g sample of kernels. The second batch was prepared by adding the remaining 815 g of kernels from the 500- to 518-µm-diameter fraction with the 518- to 534-µm-diameter fraction and subsequently thoroughly mixing and blending it with a Jones riffle splitter. Afterward, the batch was sorted into sixteen 100-g samples plus one 30-g sample of kernels in the 500- to 534-µm-diameter range. A total of 2016 g of kernels, the required milestone, were produced for coating. As a final step, each of the smaller batches was rerolled in a custom-made stainless steel rolling pan with a slit at one end to sort out and remove any out-of-round or defective kernels. Visual examination with a microscope found the kernels to have excellent sphericity and little surface roughness from the blending and riffling. There was also no visual evidence of any dusting.

A representative sample of kernels from the two batches was sent to the analytical chemistry organization at ORNL for analysis. The sample was microwave digested in ultrapure nitric acid to completely dissolve the sample. The uranium was then separated from the solution by using transuranic resin obtained from Eichrome Technology, Inc., and the collected column effluent was subsequently analyzed by ICP-MS. The only cations reported that were above the detection limit were as follows: 33.6 ± 3.4 µg/g Ni, 11.6 ± 1.2 µg/g Al, 10.7 ± 1.1 µg/g Ca, 10.6 ± 1.1 µg/g Cu, and 5.6 ± 0.6 µg/g Cr. A sample of kernels was also sent to the Materials and Chemistry Laboratory, Inc. (located at the East Tennessee Technology Park), to be analyzed for chloride via pyrohydrolysis, with the chloride content being determined by ion chromatography. The chloride value was below the detection limit of 19 µg/g.

The average particle density of a 100.026-g sample of 500- to 534-µm-diameter kernels was determined to be 10.78 g/cm^3, using a calibrated Ultrapycnometer 1000 by Quantochrome (Fig. 21). This value is about 98% of theoretical density. With the same sample, using an Autotap instrument by Quantochrome, the average tap density for three separate measurements (using 50 taps) was 6.68 g/cm^3 (Fig. 22). The slow-pour bulk density with the same sample was 6.69 g/cm^3. The average crush strength was

determined to be >1200 g. The average crush strength was determined for ten randomly picked kernels. Each kernel was placed on the analytical balance pan and under the flat smooth surface of the stainless steel rod of the crushing apparatus shown in Fig. 23. The force in grams needed to crush a kernel is defined as the crush strength for that kernel. In each measurement, force was applied slowly and smoothly to the kernel with no twisting movement. When the kernel shattered, the mass shown on the balance plummeted to zero. Between measurements, the surfaces were cleaned of broken particles. Because the upper limit for the balance was 1200 g, none of these spheres were crushed.

A 100-g sample of the 500- to 534-µm-diameter kernels was packaged and sent to Building 4508 on September 25, 2003, for use by the Metals and Ceramics Division to make the initial coating run. The remaining 100-g samples were packaged and sent to Building 4508 on January 30, 2003.

Data obtained for the Metals and Ceramics Division characterization laboratory showed that the 500-µm DUO_2 kernels had a mean diameter of 519 ± 1 µm, with less than 1% measured outside the range 500–545; a mean sphericity of 1.02 ± 0.01 µm, with less than 0.5% measured greater than 1.05; an envelope density of about 10.6 g/cm^3; and an open porosity of about 1%. Scanning electron microscopy (SEM) showed a rough kernel surface with grains less than 10 µm in size. Closed pores of 0.25-µm diameter were observed throughout the kernels.

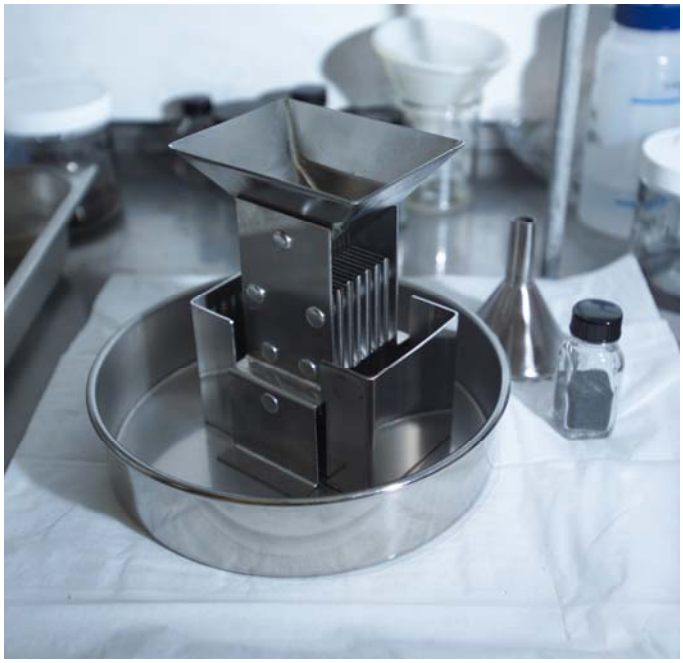

Fig. 20. Jones riffle splitter.

Fig. 21. Ultrapycnometer 1000 by Quantochrome, which was used to determine particle density of UO_2 kernels.

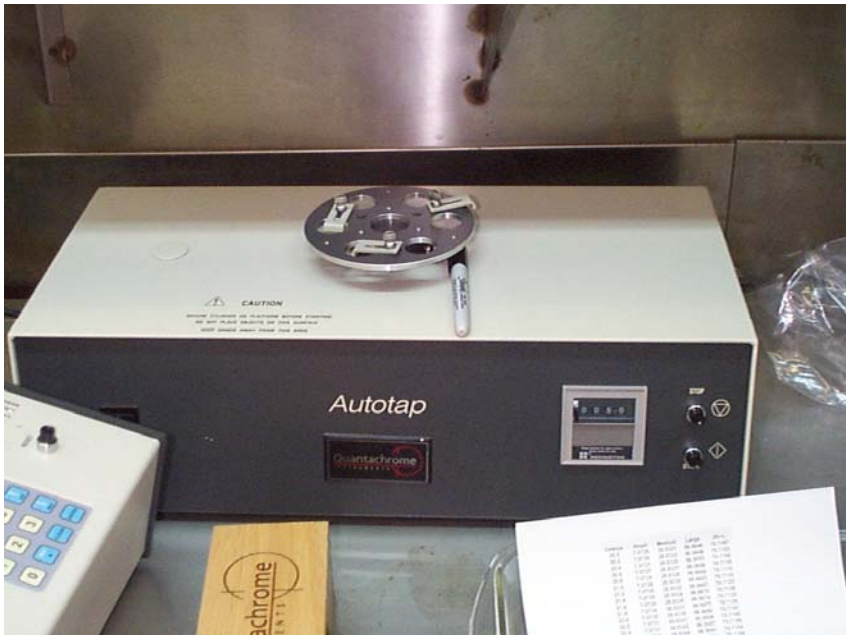

Fig. 22. Autotap instrument by Quantochrome, which was used to measure tap density of samples of UO_2 kernels.

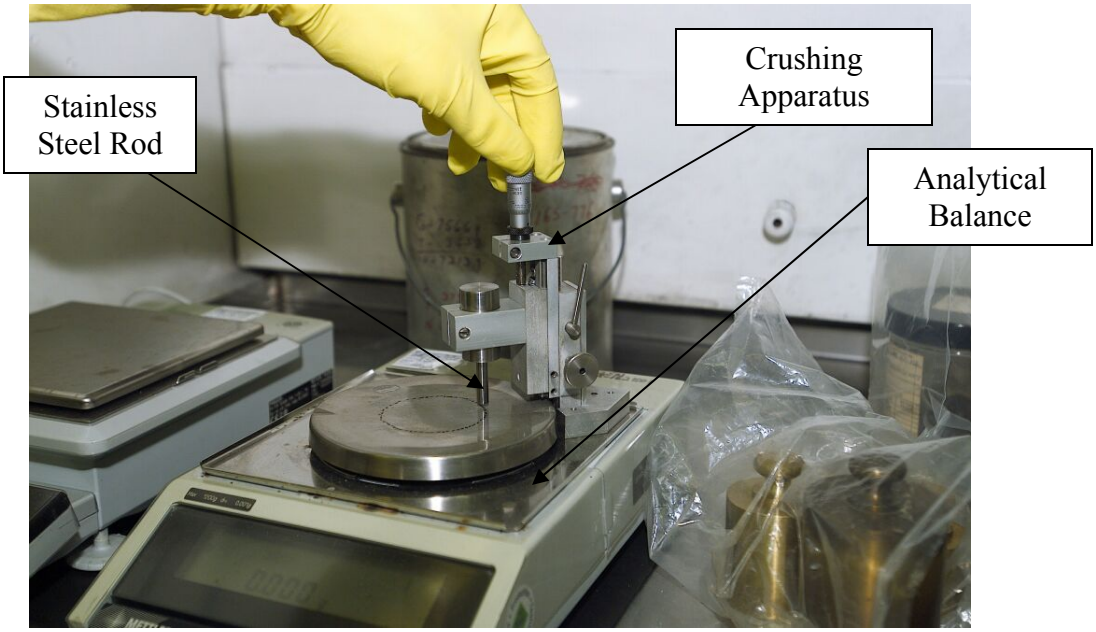

Fig. 23. Custom-designed apparatus to measure crush strength of air-dried $UO_3 \cdot 2H_2O$ spheres and calcined and sintered UO_2 kernels.

9. PRODUCTION CAMPAIGN TO PRODUCE 3.5 kg OF 350±10-µm-diameter UO_2 KERNELS

The second task of the AGR kernel production effort was to produce 3.5 kg of 350±10-µm-diameter UO_2 kernels. Following a fairly successful campaign to produce the 500-µm kernels, many operational problems were encountered in the first 2 months during the gel-forming runs and with the calcining and sintering furnace. The sieving results obtained for the air-dried $UO_3 \cdot 2H_2O$ microspheres collected in the first 24 runs are summarized in Table 5, along with the slow-pour densities. These results clearly show that operational problems were encountered that prevented high yields of targeted air-dried microspheres in the 600- to 850-µm-diameter range. Only about 66% of the microspheres produced in these runs were in this range. By comparison, 86% of the air-dried spheres obtained in the campaign to produce 500-µm kernels were on target.

In the early stages of this campaign, a problem was encountered in a few of the initial runs, in which an uncontrollable coalescing of the broth droplets occurred. The length of the slit in the stainless tube that forms the veil of silicone oil at the top of the gel-forming column was shortened to provide a smoother veil. The length of the downstream plastic tubing from the forming column was also shortened from 13 to 9 ft to increase the flow through the gel-forming system. These modifications corrected the problem.

In a few of the runs, a problem was encountered: a yellow color was observed in the 0.5 *M* NH_4OH wash solutions that was not observed in the production runs to make the 500±20-µm kernels. The outer surfaces of the gel spheres were being strangely leached by the wash solution. During this period no changes were made to the broth formulation or operating conditions. However, it was discovered that the use of TCE that

had been recycled several times through a distillation apparatus appeared to have caused the problem. This problem disappeared when new TCE or TCE that had been recycled only once was used to remove the residual silicone oil from the surfaces of the gel spheres. It was also determined that the TCE that was causing the leaching problem could be made usable by first washing it with a 0.5 *M* NH_4OH wash solution and then passing it through the distillation apparatus.

It was also very obvious in the first few runs that the quality of the broth droplet–forming needle had to be improved. Imperfections in the tip of the needles being used led to side streams, which produced an appreciable amount of very small microspheres. To correct this problem (as previously noted in this report), custom-designed stainless steel needles were purchased from Popper & Sons (see Fig. 13). The key to the design was to have a circular, burr- and crack-free, mildly electropolished, and tapered blunt-end orifice. These needles proved to be very good in providing uniform droplets and the targeted yield.

Table 5. Sieve fractions and slow-pour densities of air-dried microspheres produced in the campaign to make 350-µm-diameter kernels with the Alpha-M Corporation controller and vibrator

Run no.	Total mass of kernels collected (g)	Mass of sieve fractions (g)					Slow-pour density (g/mL)
		<600 µm	600–710 µm	710–850 µm	850–1000 µm	>1000 µm	
DUN-89	83.00	1.46	0.11	45.73	17.65	18.05	1.12
DUN-90	86.81	5.30	0.02	60.07	20.69	0.73	1.12
DUN-91	84.28	7.00	0.17	60.05	16.15	0.91	1.14
DUN-92	83.13	0.65	0.15	60.44	21.38	0.51	1.11
DUN-97	84.28	3.66	0.01	43.66	16.54	20.41	1.14
DUN-98	84.45	1.24	1.81	36.16	17.82	27.42	1.14
DUN-99	82.71	0.28	2.75	44.26	21.28	14.14	1.11
DUN-100	80.31	0.24	0.53	59.81	17.79	1.94	1.11
DUN-101	86.05	0.34	5.52	50.08	25.00	5.11	1.08
DUN-102	85.29	0.26	5.81	32.48	30.03	16.71	1.09
DUN-103	82.96	0.22	29.51	13.81	23.56	15.86	1.13
DUN-104	83.28	21.30	11.36	41.55	7.77	1.30	1.13
DUN-105	77.77	3.52	16.80	52.05	4.15	1.25	1.10
DUN-106	82.06	6.57	10.82	63.23	1.02	0.42	1.10
DUN-107	82.82	1.83	1.07	5.09	4.42	70.41	1.09
DUN-108	81.77	0.60	7.83	13.83	13.67	45.84	1.10
DUN-109	77.37	2.32	19.14	50.57	2.39	2.95	1.10
DUN-110	82.69	3.01	19.55	51.65	7.33	1.15	1.10
DUN-111	83.06	2.52	19.25	56.50	4.62	0.17	1.10
DUN-112	82.72	0.36	47.98	22.76	10.95	0.67	1.10
DUN-113	83.12	0.10	14.46	20.63	37.39	10.54	1.10
DUN-114	82.53	0.21	71.92	7.91	2.07	0.42	1.10
DUN-115	82.71	0.41	43.38	36.29	2.33	0.30	1.09
DUN-116	81.73	0.36	39.87	19.63	21.38	0.49	1.10
Total	1986.90	63.76	369.82	948.24	347.38	257.70	
		(3.21%)	(18.61%)	(47.72%)	(17.48%)	(12.97%)	

In a couple of runs, when the needle was being positioned toward the veil at the beginning of the runs, the tip of the needle with the broth droplets streaming toward the veil inadvertently touched part of the tube surface at or near the veil slit. Gelled broth on the surface of the tube caused enough disturbances in the veil flow to cause coalescing of the broth droplets. This situation was corrected when the gel was removed from the surface using specialized tools. To prevent this problem from occurring again, a stainless steel cover was made to make it difficult for the needle to touch those surfaces.

Another serious problem was encountered when the Alpha-M Corporation vibrator controller (Fig. 3) began to malfunction and became difficult to control. The first 24 runs were made with this system. Unfortunately, the Alpha-M Corporation went out of business several years ago, making it impossible to obtain a new controller or replacement parts. A different controller and vibrator system were purchased from Labworks, Inc. (Figs. 9 and 10). This equipment was used with a low-impedance accelerometer from Kistler Instrument Corporation (Fig. 11). The remaining 68 runs (Table 6) were made with this system.

The initial use of the new system also proved difficult to control. During the first seven runs, two different sizes of microspheres were predominately produced. Afterward, six good-to-excellent runs were made. The bimodal problem then returned intermittently for the next 19 runs, making it difficult to understand. The problem was thought to be in the controller, but this was not the case. Fortuitously, it was discovered that the top surface of the accelerometer had to be perfectly positioned parallel with the plastic tube and the split stainless steel tube above it (Fig. 12). Table 7 gives the results of 19 poor runs.

For these runs, 33.72% (489.51 g) and 37.34% (541 g) of the collected air-dried kernels were in the 600- to 710-μm and 850- to 1000-μm sieve fractions, with only 15.75% (228.69 g) being in the 710- to 850-μm fraction that separated them. For these poor runs, only 49.47% of the targeted 600- to 850-μm fraction was obtained.

The 710- to 850-μm fractions for runs DUN-120 and -121 were individually calcined and sintered, with the results given in Table 8. The calcining and sintering data showed that 97.5% of the DUN-120 kernels were in the targeted 332- to 368-μm-diameter range, as were ~78% of the DUN-121 kernels.

After January 30, 2004, most of the difficult operational problems encountered in earlier runs had been solved. The operation of the small-scale apparatus was optimized and provided excellent automatic control of the droplet formation. The gel spheres produced in these runs were of the highest quality. During the final 36 runs, the specified yield of air-dried product in the 600- to 850-μm range was as follows: 25 runs for 90 to 99.5%, 4 runs for 70 to 80%, 1 run for 60 to 70%, and 2 runs for less than 50%. Most of the 600- to 850-μm-diameter microspheres yielded sintered kernels that were primarily in the 342- to 359-μm range. Table 9 gives the sieve fractions and slow-pour densities of air-dried spheres of the best runs, using the Labworks automatic frequency controller and vibrator system. It also includes the good runs obtained during the period when the bimodal problem was still unresolved. A total of 68 runs were made with the new vibrating system, of which 49 (or 72%) would be considered excellent runs. For these runs, about 3751 g of the kernels (or 90%) were in the targeted 600- to 850-μm-diameter sieve range.

Table 6. Sieve fractions and slow-pour densities of air-dried spheres produced in the campaign to make 350-µm-diameter kernels with a Labworks, Inc., controller and vibrator system and Kistler Instrument Corporation accelerometer

Run no.	Total mass of kernels collected (g)	Mass of Sieve fraction (g)					Slow-pour density (g/mL)
		<600 µm	600–710 µm	710–850 µm	850–1000 µm	>1000 µm	
DUN-17	34.58	4.72	9.20	11.10	9.37	0.19	1.11
DUN-18	79.95	0.46	39.91	10.90	28.10	0.58	1.11
DUN-19	82.72	0.24	24.88	16.83	39.03	1.74	1.11
DUN-20	83.35	0.20	39.44	12.66	22.18	8.87	1.10
DUN-21	78.10	0.21	32.23	11.26	33.18	1.22	1.10
DUN-122	79.86	0.19	17.77	6.03	10.49	45.38	1.08
DUN-123	86.55	0.17	31.11	8.00	21.26	26.01	1.08
DUN-124	81.98	0.21	71.68	5.83	2.88	1.38	1.09
DUN-125	81.75	0.04	63.27	6.89	8.32	3.23	1.09
DUN-126	81.82	0.22	75.98	3.89	1.00	0.73	1.09
DUN-127	81.11	0.02	62.06	8.05	10.45	0.53	1.08
DUN-128	79.52	0.27	51.57	15.58	10.22	1.88	1.10
DUN-129	82.46	0.05	67.23	6.86	7.69	0.63	1.10
DUN-130	80.97	0.57	37.03	11.69	30.48	1.20	1.10
DUN-131	82.24	0.12	21.68	14.39	37.63	8.42	1.10
DUN-132	81.47	0.01	51.76	13.61	14.49	1.60	1.08
DUN-133	82.90	0.00	13.99	20.26	36.71	11.94	1.09
DUN-134	81.56	0.42	60.86	7.42	10.09	2.77	1.08
DUN-135	83.30	0.32	45.19	14.15	22.22	1.42	1.10
DUN-136	82.28	0.10	69.89	2.72	4.19	5.38	1.10
DUN-137	87.04	0.04	83.28	1.55	1.90	0.27	1.10
DUN-138	85.18	0.73	34.77	8.92	35.22	5.54	1.08
DUN-139	86.13	0.04	56.21	8.61	17.83	3.44	1.11
DUN-140	84.83	0.13	26.93	14.82	36.34	6.61	1.08
DUN-141	85.90	0.50	37.71	17.05	27.67	2.97	1.12
DUN-142	86.62	0.01	31.58	8.99	40.43	5.61	1.09
DUN-143	87.19	0.26	26.09	14.44	43.85	2.55	1.09
DUN-144	89.12	2.76	67.46	16.42	2.07	0.41	1.08
DUN-145	79.93	2.63	59.49	16.87	0.39	0.55	1.08
DUN-146	86.66	0.23	30.86	20.26	33.79	1.52	1.09
DUN-147	87.35	0.20	47.14	10.99	28.66	0.36	1.09
DUN-148	87.48	0.04	52.59	11.25	22.28	1.32	1.09
DUN-149	87.16	1.28	69.02	14.15	2.64	0.07	1.13
DUN-150	85.83	3.04	72.23	7.98	2.29	0.29	1.08
DUN-151	84.59	1.67	63.37	15.19	3.30	1.06	1.09
DUN-152	80.57	0.30	15.88	4.34	12.34	47.71	1.09
DUN-153	83.52	0.94	18.45	16.75	43.92	3.46	1.07
DUN-154	84.76	0.20	75.59	5.37	3.16	0.44	1.07
DUN-155	84.73	0.14	70.67	5.83	6.00	0.22	1.08
DUN-156	84.73	0.24	59.00	10.48	12.67	2.34	1.08
DUN-157	83.56	0.21	50.51	12.17	15.32	5.35	1.10
DUN-158	84.64	0.03	78.11	5.39	0.89	0.22	1.10
DUN-159	83.14	0.14	62.64	8.55	11.06	0.75	1.09
DUN-160	83.56	0.11	74.34	4.77	3.98	0.36	1.08
DUN-161	84.62	0.14	72.97	5.55	5.50	0.46	1.09
DUN-162	83.95	0.06	75.21	3.75	3.33	1.60	1.09
DUN-163	84.83	5.66	69.82	8.03	1.16	0.16	1.09
DUN-164	84.75	0.05	79.79	2.42	2.26	0.23	1.09
DUN-165	83.21	0.28	45.91	10.95	14.75	11.32	1.12
DUN-166	84.89	0.18	79.20	2.86	1.39	1.26	1.08
DUN-167	85.08	0.08	81.87	2.69	0.43	0.01	1.08
DUN-168	84.88	0.46	76.66	6.21	1.07	0.48	1.08
DUN-169	84.31	1.20	61.25	14.24	6.74	0.88	1.09
DUN-170	84.30	0.04	74.79	4.51	4.05	0.91	1.07
DUN-171	86.33	0.13	78.89	3.35	2.64	0.26	1.07
DUN-172	86.22	0.57	67.66	10.04	6.16	0.70	1.09
DUN-173	85.40	0.05	68.10	8.87	7.77	0.61	1.10
DUN-174	89.36	0.17	79.89	7.73	1.11	0.46	1.08
DUN-175	89.15	0.10	61.98	8.50	17.99	0.58	1.08
DUN-176	88.03	0.03	79.48	5.78	2.10	0.64	1.08
DUN-177	89.06	0.11	80.32	6.68	1.75	0.20	1.08
DUN-178	89.77	0.18	79.87	8.14	0.62	0.96	1.08
DUN-179	91.91	0.02	80.35	7.11	1.86	0.47	1.10
DUN-180	90.31	0.03	77.58	9.16	1.65	0.80	1.09
DUN-181	88.74	0.34	61.93	9.48	12.03	3.86	1.10
DUN-182	90.57	0.01	75.96	7.11	5.70	0.70	1.09
DUN-183	90.01	0.02	79.00	7.99	1.85	0.06	1.09
Total	5632.37	34.32 (0.61%)	3839.13 (68.16%)	630.41 (11.19%)	871.89 (15.48%)	246.13 (4.37%)	

Table 7. Sieve fractions and slow-pour densities of air-dried spheres for 19 poor runs using the Labworks, Inc., controller and vibrator and Kistler Instrument Corporation accelerometer

	Mass of sieved fraction (g)					
Run no.	<600 µm	600–710 µm	710–850 µm	850–1000 µm	>1000 µm	Slow-pour density (g/mL)
DUN-117	4.72	9.20	11.10	9.37	0.19	1.11
DUN-118	0.46	39.91	10.90	28.10	0.58	1.11
DUN-119	0.24	24.88	16.83	39.03	1.74	1.11
DUN-120	0.20	39.44	12.66	22.18	8.87	1.10
DUN-121	0.21	32.23	11.26	33.18	1.22	1.10
DUN-122	0.19	17.77	6.03	10.49	45.38	1.08
DUN-123	0.17	31.11	8.00	21.26	26.01	1.08
DUN-130	0.57	37.03	11.69	30.48	1.20	1.10
DUN-131	0.12	21.68	14.39	37.63	8.42	1.10
DUN-133	0.00	13.99	20.26	36.71	11.94	1.09
DUN-138	0.73	34.77	8.92	35.22	5.54	1.08
DUN-140	0.13	26.93	14.82	36.34	6.61	1.08
DUN-141	0.50	37.71	17.05	27.67	2.97	1.12
DUN-142	0.01	31.58	8.99	40.43	5.61	1.09
DUN-143	0.26	26.09	14.44	43.85	2.55	1.09
DUN-146	0.23	30.86	20.26	33.79	1.52	1.09
DUN-152	0.30	15.88	4.34	12.34	47.71	1.09
DUN-153	0.94	18.45	16.75	43.92	3.46	1.07
Total	9.98	489.51	228.69	541.99	181.52	
	(0.69%)	(33.72%)	(15.75%)	(37.34%)	(12.5%)	

Table 8 shows that the 600- to 850-µm-diameter sieve fractions that were calcined and sintered for these runs resulted in sintered spheres in the targeted 332–358-µm range, about 80% of which were in the 342–359-µm range. Table 10 provides the calcining and sintering product data for the period of time in which most of the poor runs occurred. About 573 g (or 37.4%) of the calcined and sintered kernels were in the 342–359-µm range; about 59.4% (911 g) were in the 332–358-µm range. Table 11 describes the calcined and sintered kernels for most of the good runs. For these runs, ~2855 g (or 81.9%) of the calcined and sintered kernels were in the 342–359-µm range and 91.2% (3179 g) were in the 332–358-µm range. All the gel-forming operational improvements made dramatic improvements in the targeted kernels yields.

Once the last of the air-dried product was calcined, sintered, sieved, and rolled to remove any defective kernels, the fractions of 332–342-µm- (263 g), 342–359-µm- (3403 g), and 359–368-µm- (502 g) diameter were separately combined and thoroughly mixed. Each of the composite fractions was then sieved again with the precision sieves and rerolled. The final inventory of 332–368-µm-diameter kernels was 4001.35 g with the following distribution: 332–342 µm (200.18 g), 342–359 µm (3400.99 g), and 359–368 µm (500.18 g). About 85% of the kernels were in the 342–359-µm-diameter range.

Table 8. Sieve data for UO_2 kernels obtained after calcining and sintering the 600- to 850-µm-diameter fractions of air-dried spheres

Batch	Mass per batch (g)	Mass of sieved fraction (g)					
		<332 µm	332–342 µm	342–359 µm	359–368 µm	368–425 µm	>425 µm
DUN-89, 90, 91, 97, 98	318.01	0.01	62.85	125.63	36.31	93.01	0.20
DUN-92	46.53	0.02	0.20	27.52	11.31	2.95	4.53
1[a]	225.58	64.85	48.61	85.17	20.48	6.08	0.39
2[a]	187.33	50.02	41.05	72.20	18.58	5.09	0.39
DUN-100	50.62	0.00	0.08	0.12	1.53	47.84	1.05
DUN-101	45.73	0.19	0.31	2.37	3.67	38.94	0.25
DUN-102	33.78	0.02	0.21	5.56	4.70	23.10	0.19
DUN-103	35.04	0.05	0.18	6.43	15.88	11.92	0.58
DUN-104	43.28	4.77	0.12	1.92	6.19	27.30	2.98
DUN-105	58.08	0.46	0.85	9.87	9.70	36.83	0.37
DUN-106	60.20	0.25	0.29	2.65	9.43	47.52	0.06
DUN-109, 110, 113, 114, 115, 116, 118	132.93	0.65	4.38	83.86	19.99	14.25	9.80
DUN-120	42.59	0.04	0.10	40.87	0.55	0.42	0.61
DUN-121	36.02	0.48	0.40	26.86	0.79	1.31	6.18
DUN-122, 123, 125	124.97	1.15	1.32	109.57	2.06	2.43	8.44
DUN-111, 112, 124	139.32	0.34	3.06	66.77	8.36	46.02	14.77
DUN-124, 128, 129	137.32	1.03	6.50	110.41	2.44	3.59	13.35
DUN-99, 107, 108, 111, 119, 127	158.52	0.13	0.39	83.20	9.29	47.30	18.21
DUN-130, 131, 132, 133	147.78	1.33	7.60	95.30	3.41	4.41	35.73
DUN-117, 126, 134, 135	192.27	1.95	4.58	153.01	7.68	7.08	17.97
DUN-136, 137	129.91	0.06	0.50	125.33	1.98	0.80	1.24
DUN-138, 139, 140, 141	133.62	0.26	3.01	95.99	5.81	4.05	24.50
DUN-142, 143, 144, 145	199.77	0.96	5.42	138.22	25.06	17.33	12.78
DUN-146, 147, 148, 149	211.70	3.13	6.56	123.01	47.40	14.55	17.05
DUN-150, 151	131.28	0.74	14.64	90.83	17.28	3.87	3.92
DUN-152, 153, 154, 155	175.54	0.69	3.72	149.51	8.98	6.16	6.48
DUN-156, 157, 158, 159, 160, 161	366.53	0.26	1.84	330.87	10.74	4.71	18.11
DUN-162, 163, 164, 165, 166	311.18	2.59	16.94	263.97	12.74	5.15	9.79
DUN-167, 168, 169, 170, 171	333.08	1.34	7.14	293.34	18.35	6.77	6.14
DUN-172, 173, 174, 175	257.10	0.78	2.23	215.01	25.83	3.61	9.64
DUN-176, 177, 178, 179	286.33	0.10	0.59	269.72	12.55	2.15	1.22
DUN-180, 181, 182, 183	269.17	0.14	0.92	222.85	36.99	4.85	13.42
Total	4751.94	138.65	245.67	3205.09	379.07	536.54	246.92
		(2.92%)	(5.17%)	(67.45%)	(7.98%)	(11.29%)	(5.20%)

[a]Contains 600- to 850-µm-diameter fractions of air-dried spheres from runs DUN-29 through -41, which were conducted in the AAA Program.

A representative sample of these kernels was sent to analytical chemistry at ORNL for ICP-MS analysis. The results were as follows: 15.6 ± 1.6 µg/g K, 13.4 ± 1.3 µg/g Cr, 6.3 ± 0.6 µg/g Fe, 5.4 ± 0.4 µg/g Mg, 5.1 ± 0.5 µg/g Al, 4.5 ± 0.5 µg/g Ni, and 2.7 ± 0.3 µg/g Cu. All the other cations given were either <1 µg/g or below the detection limit. Lithium was measured at below the detection limit of 0.26 µg/g. A separate sample of kernels was analyzed by the Materials and Chemistry Laboratory, Inc. (located at the East Tennessee Technology Park), for chloride by pyrohydrolysis/ion-chromatography analysis. The Chloride values for duplicate samples were <35 and <19 µg/g.

Table 9. Sieve fractions and slow-pour densities of air-dried spheres of the best runs using the Labworks, Inc., controller and vibrator and Kistler Instrument Corporation accelerometer

	Mass of sieved fraction (g)					
Run no.	<600 µm	600–710 µm	710–850 µm	850–1000 µm	>1000 µm	Slow-pour density (g/mL)
DUN-124	0.21	71.68	5.83	2.88	1.38	1.09
DUN-125	0.04	63.27	6.89	8.32	3.23	1.09
DUN-126	0.22	75.98	3.89	1.00	0.73	1.09
DUN-127	0.02	62.06	8.05	10.45	0.53	1.08
DUN-128	0.27	51.57	15.58	10.22	1.88	1.10
DUN-129	0.05	67.23	6.86	7.69	0.63	1.10
DUN-132	0.01	51.76	13.61	14.49	1.60	1.08
DUN-134	0.42	60.86	7.42	10.09	2.77	1.08
DUN-135	0.32	45.19	14.15	22.22	1.42	1.10
DUN-136	0.10	69.89	2.72	4.19	5.38	1.10
DUN-137	0.04	83.28	1.55	1.90	0.27	1.10
DUN-139	0.04	56.21	8.61	17.83	3.44	1.11
DUN-144	2.76	67.46	16.42	2.07	0.41	1.08
DUN-145	2.63	59.49	16.87	0.39	0.55	1.08
DUN-147	0.20	47.14	10.99	28.66	0.36	1.09
DUN-148	0.04	52.59	11.25	22.28	1.32	1.09
DUN-149	1.28	69.02	14.15	2.64	0.07	1.13
DUN-150	3.04	72.23	7.98	2.29	0.29	1.08
DUN-151	1.67	63.37	15.19	3.30	1.06	1.09
DUN-154	0.20	75.59	5.37	3.16	0.44	1.07
DUN-155	0.14	70.67	5.83	6.00	0.22	1.08
DUN-156	0.24	59.00	10.48	12.67	2.34	1.08
DUN-157	0.21	50.51	12.17	15.32	5.35	1.10
DUN-158	0.03	78.11	5.39	0.89	0.22	1.10
DUN-159	0.14	62.64	8.55	11.06	0.75	1.09
DUN-160	0.11	74.34	4.77	3.98	0.36	1.08
DUN-161	0.14	72.97	5.55	5.50	0.46	1.09
DUN-162	0.06	75.21	3.75	3.33	1.60	1.09
DUN-163	5.66	69.82	8.03	1.16	0.16	1.09
DUN-164	0.05	79.79	2.42	2.26	0.23	1.09
DUN-165	0.28	45.91	10.95	14.75	11.32	1.12
DUN-166	0.18	79.20	2.86	1.39	1.26	1.08
DUN-167	0.08	81.87	2.69	0.43	0.01	1.08
DUN-168	0.46	76.66	6.21	1.07	0.48	1.08
DUN-169	1.20	61.25	14.24	6.74	0.88	1.09
DUN-170	0.04	74.79	4.51	4.05	0.91	1.07
DUN-171	0.13	78.89	3.35	2.64	0.26	1.07
DUN-172	0.57	67.66	10.04	6.16	0.70	1.09
DUN-173	0.05	68.10	8.87	7.77	0.61	1.10
DUN-174	0.17	79.89	7.73	1.11	0.46	1.08
DUN-175	0.10	61.98	8.50	17.99	0.58	1.08
DUN-176	0.03	79.48	5.78	2.10	0.64	1.08
DUN-177	0.11	80.32	6.68	1.75	0.20	1.08
DUN-178	0.18	79.87	8.14	0.62	0.96	1.08
DUN-179	0.02	80.35	7.11	1.86	0.47	1.10
DUN-180	0.03	77.58	9.16	1.65	0.80	1.09
DUN-181	0.34	61.93	9.48	12.03	3.86	1.10
DUN-182	0.01	75.96	7.11	5.70	0.70	1.09
DUN-183	0.02	79.00	7.99	1.85	0.06	1.09
Total	24.34	3349.62	401.72	329.90	64.61	
	(0.58%)	(80.32%)	(9.63%)	(7.91%)	(1.55%)	

Table 10. Sieve data for UO_2 kernels obtained after calcining and sintering the 600- to 850-µm-diameter fractions of air-dried spheres from operations with a large number of poor runs

Batch	Mass per batch (g)	Mass of sieved fraction (g)					
		<332 µm	332–342 µm	342–359 µm	359–368 µm	368–425 µm	>425 µm
DUN-98	318.01	0.01	62.85	125.63	36.31	93.01	0.20
DUN-92	46.53	0.02	0.20	27.52	11.31	2.95	4.53
1[a]	225.58	64.85	48.61	85.17	20.48	6.08	0.39
2[a]	187.33	50.02	41.05	72.20	18.58	5.09	0.39
DUN-100	50.62	0.00	0.08	0.12	1.53	47.84	1.05
DUN-99, 107, 108, 111, 119, 127	158.52	0.13	0.39	83.20	9.29	47.30	18.21
DUN-111, 112, 124	139.32	0.34	3.06	66.77	8.36	46.02	14.77
DUN-101	45.73	0.19	0.31	2.37	3.67	38.94	0.25
DUN-102	33.78	0.02	0.21	5.56	4.70	23.10	0.19
DUN-103	35.04	0.05	0.18	6.43	15.88	11.92	0.58
DUN-104	43.28	4.77	0.12	1.92	6.19	27.30	2.98
DUN-105	58.08	0.46	0.85	9.87	9.70	36.83	0.37
DUN-106	60.20	0.25	0.29	2.65	9.43	47.52	0.06
DUN-109, 110, 113, 114, 115, 116, 118	132.93	0.65	4.38	83.86	19.99	14.25	9.80
Total	1534.95	121.76	162.58	573.27	175.42	448.15	53.77
		(7.93%)	(10.59%)	(37.35%)	(11.43%)	(29.20%)	(3.50%)

[a]Contains 600- to 850-µm-diameter fractions of air-dried spheres from runs DUN-29 through -41, which were conducted in the AAA Program.

Table 11. Sieve data for UO_2 kernels obtained after calcining and sintering the 600- to 850-µm-diameter fractions of air-dried spheres from the operations with primarily good runs

Batch	Mass per batch (g)	Mass of sieved fraction (g)					
		<332 µm	332–342 µm	342–359 µm	359–368 µm	368–425 µm	>425 µm
DUN-120	42.59	0.04	0.10	40.87	0.55	0.42	0.61
DUN-121	36.02	0.48	0.40	26.86	0.79	1.31	6.18
DUN-122, 123, 125	124.97	1.15	1.32	109.57	2.06	2.43	8.44
DUN-124, 128, 129	137.32	1.03	6.50	110.41	2.44	3.59	13.35
DUN-130, 131, 132, 133	147.78	1.33	7.60	95.30	3.41	4.41	35.73
DUN-117, 126, 134, 135	192.27	1.95	4.58	153.01	7.68	7.08	17.97
DUN-136, 137	129.91	0.06	0.50	125.33	1.98	0.80	1.24
DUN-138, 139, 140, 141	133.62	0.26	3.01	95.99	5.81	4.05	24.50
DUN-142, 143, 144, 145	199.77	0.96	5.42	138.22	25.06	17.33	12.78
DUN-146, 147, 148, 149	211.70	3.13	6.56	123.01	47.40	14.55	17.05
DUN-150, 151	131.28	0.74	14.64	90.83	17.28	3.87	3.92
DUN-152, 153, 154, 155	175.54	0.69	3.72	149.51	8.98	6.16	6.48
DUN-156, 157, 158, 159, 160, 161	366.53	0.26	1.84	330.87	10.74	4.71	18.11
DUN-162, 163, 164, 165, 166	311.18	2.59	16.94	263.97	12.74	5.15	9.79
DUN-167, 168, 169, 170, 171	333.08	1.34	7.14	293.34	18.35	6.77	6.14
DUN-172, 173, 174, 175	257.10	0.78	2.23	215.01	25.83	3.61	9.64
DUN-180, 181, 182, 183	269.17	0.14	0.92	222.85	36.99	4.85	13.42
Total	3486.16	17.03	84.01	2854.67	240.64	93.24	196.57
		(0.49%)	(2.41%)	(81.89%)	(6.90%)	(2.67%)	(5.64%)

Using one of the 100-g samples of 342–359-µm-diameter kernels, the average kernel density was determined via the Ultrapycnometer 1000 (Fig. 21) to be 10.85 g/cm^3. The average tap density for this sample of kernels was determined to be 6.65 g/cm^3, using the Autotap shown in Fig. 22. The slow-pour density was 6.69 g/cm^3. A cursory microscopic examination of kernels showed excellent sphericity, minimal surface roughness, and no evidence of cracking. The final characterization will be performed by the Metals and Ceramics Division.

The final task of the production campaign was to subdivide the three fractions into 100-g samples in glass bottles and package them into forty 1-qt metal cans as shown in Fig. 24.

Fig. 24. Forty 1-qt metal cans each containing 100-g samples of UO_2 kernels for transfer to the Metals and Ceramics Division.

10. EXAMPLE OF AN IDEAL RUN

During the campaign to produce 3.5 kg of UO_2 kernels with a diameter of 350 ± 10 μm, a large number of ideal gel-forming runs were made, especially during the last 36 runs. Run DUN-179 is representative of these runs. This run was conducted under optimum control using all the lessons learned during the two campaigns and is an excellent example of how to ideally use the internal gelation process to prepare UO_2 kernels. The run data sheets in Figs. 25 and 26 provide all the key data about run DUN-179, which include broth formulation, run conditions, droplet formation and control, gelation time, run time, aging time, washing steps, leaching behavior, air-drying, sieving data, slow-pour density, and crush strength.

Run DUN-179 and its companion run DUN-178 were performed on March 3, 2004. Both of these runs produced high yields of targeted product. The broth used had the following composition: 1.31 *M* U, 1.71 *M* HMTA, 1.71 *M* urea, and 2.1 *M* NO_3^-. The silicone oil was maintained at 60°C. Uniform droplets of ~1100 μm were formed using a vibrator frequency of 221.6 cycles/s (13,296 cycles/min). To check the frequency, the strobe light was set at ¼ setting, or 3325 cycles/min, to observe the stream of droplets, which appeared stationary with no side streams. Upon making contact with the hot silicone oil, the clear broth droplets began to gel in 3 to 4 s. The run lasted ~22 min, with a broth flow rate to the needle of ~9.3 mL/min. After collection, the gel spheres were aged for 20 min. After the basket was removed from the hot oil, the silicone oil was allowed to drain from the surfaces of the gel spheres for ~15 min. After four TCE washes (Fig. 25), the estimated volume of spheres was ~377 mL. The spheres were then washed six times (~30 min each) with 0.5 *M* NH_4OH to remove the HMTA, urea, and NH_4NO_3. The conductivity of each wash solution was measured. Figure 27 shows the change in conductivity for run DUN-179, which was very similar to all the other runs conducted in both campaigns. The conductivity changed from 40,240 μS for the first wash to 783 μS for the last wash. The conductivity of the stock solution was ~800 μS. Each of the wash solutions was also colorless, indicating that no surface erosion occurred during the washes. The final estimated volume of spheres was ~369 mL.

The wet gel spheres were placed in a stainless steel pan and air-dried for ~21 h with a heat lamp positioned ~2 ft above the pan. The sieving results are given in Fig. 26, which is the second page of the data summary sheet. Of the 89.77 g of air-dried spheres obtained for the run, 87.46 g of the spheres were in the targeted diameter sieve size range of 600 to 850 μm, representing a 97.43% yield. The slow-pour density of the 600- to 710-μm-diameter air-dried spheres was 1.10 g/mL (5.257 g/4.8 mL). This means that the total volume of the wet gel spheres shrank from ~369 to ~99 mL during the drying step, a factor of 3.7.

The of 600- to 850-μm-diameter air-dried spheres from runs DUN-176, -177, -178, and -179 were calcined and sintered together. A total of 286.33 g of sintered UO_2 kernels were obtained, of which 269.7 g, or 94.2%, were in the 350±10-μm range. For the four runs, 347 g, or 97.3%, of the 356.6 g of air-dried spheres collected were in the 600- to 850-μm-diameter range. Once sintered as kernels, ~98% of these spheres (282.9 g) were in the 350±20-μm-diameter range. DUN-179 and the other three runs were extremely good runs, which produced an almost perfectly targeted yield.

RUN DATA SHEET (page 1)
Date: 3/1/04 **Run Number: DUN-179**

Broth Stock Solutions

HMTA & Urea stock #: 5	Uranium stock #: UNF-11
HMTA molarity (mol/L): 3.2	U molarity (mol/L): 2.82
Urea molarity (mol/L): 3.2	U (g/L): 670.7
Density (g/mL): 1.14	$NO_3^!$/U: 1.6
	Density (g/mL): 1.86

Amounts of Stock Solutions Used to Make
Mass of U stock: 185.6 g (100 mL)
Mass of HMTA&Urea stock : 130.6 g (114.6 mL)
Total mass and volume: 316.2 g (214.6 mL)

Broth Characteristics

	(mmol)	(mmol/mL)	(mol ratio)
U	282	1.31	$NO_3^!$/U: 1.6
HMTA	366.6	1.71	HMTA/U: 1.3
Urea	366.6	1.71	Urea/U: 1.3
$NO_3^!$	351.2	2.1	HMTA/$NO_3^!$: 0.81

Temperature of Silicone Oil (within ±2°C)
Reservoir: 60°C
Veil: 60°C
Brothpot: 60°C
Inside forming column: 60°C

Drop Formation System Readings
Frequency: 221.6 cycles/s
Output: 60%
Acceleration: 3.8 to 2.7
Amp: 1.5 to 0.8
Gage of Needle: 21
Angle of needle: 40°
Needle distance: 1 - 1.5 cm
Pump set: 45 (~9.8 mL/min)
Strobe set @ 3,320 or [1/4(13,280 cycles/min)]

Run and Aging Times

	Start	End	Net
Run Time:	10:30	10:52	22 min
Aging Time:	10:53	11:13	20 min

Observations
Gelation time was 3 to 4 seconds. The run was very good with uniform droplet formation.

Fig. 25. Run data sheet for run DUN-179 (page 1)

TCE Washes

	Start	End	Net
1st TCE Wash	11:28	11.43	15 min
2nd TCE Wash	11:43	12:00	17 min
3rd TCE Wash	12:00	12:15	15 min
4th TCE Wash	12:15	12:40	25 min

Est. Bead Volume: ~377 mL

NH_4OH Washes

(Conductance of 0.5 *M* NH_4OH wash solution was [~800 μsiemens (μS)]

	Start	End	Net (min)	Conductance (μS)	Solids in wash
1st NH_4OH Wash	12:40	13:10	30	40,240	colorless
2nd NH_4OH Wash	13:10	13:40	30	22,170	colorless
3rd NH_4OH Wash	13:40	14:15	35	9,630	colorless
4th NH_4OH Wash	14:15	14:45	30	3,656	colorless
5th NH_4OH Wash	14:45	15:10	25	1,490	colorless
6th NH_4OH Wash	15:10	15:40	30	783	colorless

Bead Volume: ~369 mL

Uranium Drying and Sieving Data

Date/Time: 3/1/04
Type Drying: air-drying using heat lamp
Start Time: 16:30 (3/1/04)
End Time: 14:00 (3/2/04)

Sieve fraction (μm)	Mass (g)
>1400	0.26
1000 – 1180	0.17
850 – 1000	1.86
710 - 850	7.11
600 - 710	80.35
500 - 600	0.00
420 - 500	0.01
<420	0.01
Total	89.77

Note: 87.46 g were in the targeted diameter sieve size range of 600 to 850 μm representing 97.43 % yield. The slow pour density of (600 to 710 um) air-dried spheres was 1.10 g/mL or (5.257 g/4.8 mL). This means that the total volume of the wet gel spheres shrank from ~369 mL to ~99 mL during the drying step. The average crush strength of the air-dried kernels was 600 g.

Fig. 26. Run data sheet for run DUN-179 (page 2).

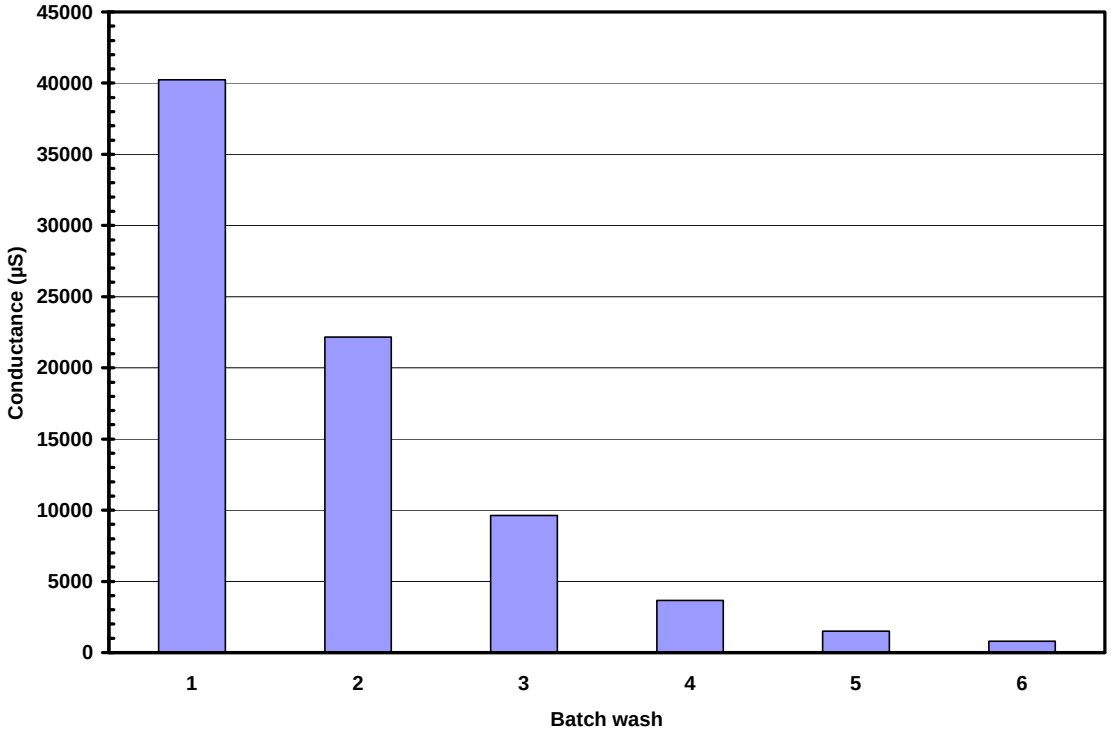

Fig. 27. Conductivity measurements of 0.5 *M* NH_4OH wash solutions used to remove reaction products from $UO_3 \cdot 2H_2O$ gel spheres in run DUN-179.

11. SUMMARY

The goals described in Sect. 1.1 for the Depleted UO_2 Kernels Production Task were accomplished. A total of 45 gel-forming preparations were made to produce 2 kg of the UO_2 kernels, which were then combined into two lots. A total of 1630 g of kernels were sieved between 500 ± 2 µm and 534 ± 2 µm with ASTM E161 electro-formed sieves, while 386 g were sieved between 482 ± 2 µm and 518 ± 2 µm (also with ASTM E161 electroformed sieves). Both batches of kernels were separately mixed well and riffled into 100-g samples. One of the samples (DUN 500-S-1) from the larger batch was analyzed by the Metals and Ceramics Division characterization laboratory at ORNL. The kernels had an average mean diameter of 519 µm, with a standard deviation in the distribution of 12 µm. In terms of variable sampling, the mean diameter of the 1.6-kg batch of kernels should be 519 ± 1 µm with 95% confidence, with <1% measured outside the range 500–545 µm. The average sphericity was 1.020 with a standard deviation of 0.008. In terms of variable sampling, the mean sphericity of the 1.6-kg batch of kernels should be 1.02 ± 0.01 µm with 95% confidence. The distribution was skewed toward higher sphericity, with <0.5% of the measured kernels having a sphericity >1.05. The envelope density, as measured with a mercury porosimeter, was 10.6 g/cm^3 with an open porosity of ~1%. The skeletal density, which was measured with a helium pycnometer, was 10.82 ± 0.16 g/cm^3. The average values for the tap and slow-pour densities were 6.68 and 6.69 g/cm^3, respectively.

Ninety-two production runs were made to obtain 3.4 kg of the 350±10-µm-diameter kernels. For the broader size diameter tolerance of 350 ± 20 µm, about 4 kg of kernels were produced. The average skeletal density for a sample of the kernels, which was measured with a helium pycnometer, was 10.85 g/cm^3 (~99% of the theoretical density). The average slow-pour density was 6.69 g/cm^3.

Analyses for cations and chloride in samples of kernels from each of the campaigns found that the concentrations of the contaminants were well within the final acceptance criterion of ≤50 µg/g. For a sample of 500-µm kernels, the only cations reported that were above the detection limit were as follows: 33.6 ± 3.4 µg/g Ni, 11.6 ± 1.2 µg/g Al, 10.7 ± 1.1 µg/g Ca, 10.6 ± 1.1 µg/g Cu, and 5.6 ± 0.6 µg/g Cr. For a sample of 350-µm kernels, detection limits were exceeded as follows: 15.6 ± 1.6 µg/g K, 13.4 ± 1.3 µg/g Cr, 6.3 ± 0.6 µg/g Fe, 5.4 ± 0.4 µg/g Mg, 5.1 ± 0.5 µg/g Al, 4.5 ± 0.5 µg/g Ni, and 2.7 ± 0.3 µg/g Cu. In separate analyses for chloride of samples of the 500- and 350-µm kernels, the concentrations were in the acceptable range, with the highest value being 35 µg/g. These cation values are near to or less than the concentrations of these cations in the ADUN stock solutions used to prepare the gel spheres.

This report also includes improvements and best past practices for uranium kernel formation via the internal gelation process, which utilizes HMTA and urea. Improvements were made in broth formulation and broth droplet formation and control that made it possible in many of the runs in the campaign to produce the 350±10-µm-diameter kernels and to obtain very high yields (>90%).

12. REFERENCES

1. F. W. van der Brugghens, A. J. Noothout, M. E. A. Hermans, J. B. W. Kanij, and O. Votocek, "A U(VI)-Process for Microsphere Production," in *Proc. Symp. Sol-Gel Processes and Reactor Fuel Cycles, Gatlinburg, Tennessee, May 4–7, 1970,* CONF-700502, U.S. Atomic Energy Commission, 1970.
2. M. H. Lloyd, K. Bischoff, K. Peng, H. U. Nissen, and R. Wessicken, "Crystal Habit and Phase Attribution of U(VI) Oxides in a Gelation Process," *J. Inorg. Nucl. Chem.* **38**, 1141–47 (1976).
3. F. J. Homan, T. B. Lindemer, E. L. Long, Jr., T. N. Tiegs, and R. L. Beatty, "Stoichiometric Effect on Performance of High-Temperature Gas-Cooled Reactor Fuels from the UCO System," *Nucl. Technol.* **35**, 428–41 (September 1977).
4. T. B. Lindemer, E. L. Long, Jr., and R. L. Beatty, "Pyrolytic Carbon-Coated Nuclear Fuel," U.S. Patent No. 4,077,838, March 7, 1978.
5. P. A. Haas, J. M. Begovich, A. D. Ryon, and J. S. Vavruska, "Chemical Flowsheet Conditions for Preparing Urania Spheres by Internal Gelation," *Ind. Eng. Chem. Prod. Res. Dev.* **19**(3), 459–67 (1980).
6. D. P. Stinton, "Mixed Uranium Dicarbide and Uranium Dioxide Microspheres and Process of Making Same," U.S. Patent No. 4,367,184, January 4, 1983.
7. M. H. Lloyd, "Coprocessed Nuclear Fuels Containing (U,Pu) Values as Oxides, Carbides, and Carbonitrides," U.S. Patent No. 4,397,778, August 9, 1983.
8. M. H. Lloyd, J. L. Collins, R. L. Fellows, S. E. Shell, D. H. Newman, and W. B. Stines, *A Gel Sphere Process for FBR Fuel Fabrication from Coprocessed Feed*, ORNL/TM-8399, Oak Ridge National Laboratory, Oak Ridge, Tenn., February 1983.
9. J. L. Collins, M. F. Lloyd, and R. L. Fellows, *Effects of Process Variables on Reaction Mechanisms Responsible for ADUN Hydrolysis, Precipitation, and Gelation in the Internal Gelation Gel-Sphere Process*, ORNL/TM-8818, Oak Ridge National Laboratory, Oak Ridge, Tenn., April 1984.
10. M. H. Lloyd, J. L. Collins, and S. E. Shell, "Method of Controlling Crystallite Size in Nuclear-Reactor Fuels," U.S. Patent No. 4,502,987, March 5, 1985.
11. J. L. Collins, M. F. Lloyd, and R. L. Fellows, "The Basic Chemistry Involved in the Internal-Gelation Method of Precipitating Uranium as Determined by pH Measurements," *Radiochim. Acta* **42**, 121–34 (1987).
12. P. A. Haas, V. L. Fowler, and M. H. Lloyd, "Preparation of Nuclear Spheres by Floatation-Internal Gelation," U.S. Patent No. 4,663,093, May 5, 1987.
13. P. A. Haas, "Formation of Uniform Liquid Drops by Application of Vibration to Laminar Jets," *Ind. Eng. Chem. Res.* **31**(3), 359–67 (1992).
14. P. A. Haas, "A New Apparatus for Continuous Countercurrent Flow of Solids and Liquids," *Sep. Sci. Technol.* **28**(8), 1579–94 (1993).
15. R. D. Spence, V. L. Fowler, and A. D. Ryon, *Equipment for Laboratory-Scale Production of (U,Pu)O_2 Spheres by the Internal Gelation Process Using Silicone Oil*, ORNL/TM-8696, Oak Ridge National Laboratory, Oak Ridge, Tenn., 1983.
16. B. B. Spencer and M. E. Whatley, *Determination of Nitric Acid and Uranium Concentrations in Aqueous Solution from Measurements of Electrical Conductivity, Density, and Temperature*, ORNL/TM-11365, Oak Ridge National Laboratory, Oak Ridge, Tenn., November 1990.

17. P. A. Haas, J. M. Begovich, A. D. Ryon, and S. J. Vavruska, *Chemical Flowsheet for Preparing Urania Spheres by Internal Gelation*, ORNL/TM-6850, Oak Ridge National Laboratory, Oak Ridge, Tenn., July 1979.
18. W. Davies and W. Gray, "Rapid and Specific Volumetric Method for Precise Determination of Uranium Using Ferrous Sulfate as Reductant," *Talanta* **11**, 1203 (1964).
19. J. L. Collins, "Method of Preparing Hydrous Titanium Oxide Gels and Spherules," U.S. Patent No. 5,821,186, October 13, 1998.
20. J. L. Collins and J. S. Watson, *Economic Evaluation for the Production of Sorbents and Catalysts Derived from Hydrous Titanium Oxide Microspheres Prepared by the HMTA Internal Gelation Process*, ORNL/TM-1999/212, Oak Ridge National Laboratory, Oak Ridge, Tenn., April 2000.
21. J. L. Collins, R. J. Lauf, and K. K. Anderson, "Method of Preparing Hydrous Iron Oxide Gels and Spherules," U.S. Patent No. 6,599,493 B2, July 29, 2003.
22. J. L. Collins, "Method of Preparing Hydrous Zirconium Oxide Gels and Spherules," U.S. Patent No. 6,602,919 B1, August 5, 2003.

ELECTRONIC DISTRIBUTION

Gary Bell, Oak Ridge National Laboratory
Jeff Binder, Oak Ridge National Laboratory
Jack Collins, Oak Ridge National Laboratory
Emory Collins, Oak Ridge National Laboratory
Guillermo Del Cul, Oak Ridge National Laboratory
Madeline Feltus, U.S. Department of Energy
Charles Forsberg, Oak Ridge National Laboratory
Sherrell Greene, Oak Ridge National Laboratory
Jeff Halfinger, BWXT Y12
David J. Hill, Oak Ridge National Laboratory
Dick Hobbins, RRH Consulting
Frank Homan, PAI Corporation
John Hunn, Oak Ridge National Laboratory
Rodney Hunt, Oak Ridge National Laboratory
Alan Icenhour, Oak Ridge National Laboratory
Andrew Kercher, Oak Ridge National Laboratory
Bob Korenke, Idaho National Engineering and Environmental Laboratory
Terry Lindemer, Harbach Engineering
Ben Lewis, Oak Ridge National Laboratory
Doug Lee, Oak Ridge National Laboratory
Rick Lowden, Oak Ridge National Laboratory
Gordon Michaels, Oak Ridge National Laboratory
Bob Morris, Oak Ridge National Laboratory
David Moses, Oak Ridge National Laboratory
Jan Palmer, Oak Ridge National Laboratory
Peter Pappano, Oak Ridge National Laboratory
David Petti, Idaho National Engineering and Environmental Laboratory
Jim Rushton, Oak Ridge National Laboratory
Roger Spence, Oak Ridge National Laboratory
Barry Spencer, Oak Ridge National Laboratory
Ken Thoms, Oak Ridge National Laboratory
Lloyd Turner, Oak Ridge National Laboratory
David Williams, Oak Ridge National Laboratory
Bob Wham, Oak Ridge National Laboratory